N-Porphyrinylamino and -amido Compounds by Addition of an Amino or Amido Nitrogen to a Porphyrin Meso Position

K. Jayaraj,[†] A. Gold,*[,†] L. M. Ball,[†] and P. S. White[‡]

Department of Environmental Sciences and Engineering and Department of Chemistry, The University of North Carolina at Chapel Hill, Chapel Hill, North Carolina 27599

Received February 3, 2000

This report describes the synthesis and characterization of a series of octaethylporphyrin derivatives in which the porphyrin π-network is connected to phenyl, 3-fluoranthenyl, or 1-pyrenyl aromatic systems through a meso amino or amido nitrogen. Metal-free bases and zinc(II) and iron(III) complexes have been obtained. These compounds represent the first examples of linkages between porphyrins and extended π-networks through a nitrogen atom directly attached to a porphyrin meso position. ^{1}H NMR studies of the metal-free bases and zinc complexes showed that in the amido-linked adducts, the plane containing the aryl substituent was oriented perpendicular to the plane of the porphyrin. Linkage through the secondary amino nitrogen, however, allowed the aryl plane to rotate toward coplanarity with the porphyrin plane, resulting in conjugation of the highest occupied aryl and porphyrin molecular orbitals through the nitrogen lone pair. In developing routes to the amino-linked compounds, the facile formation of fused azaaryl chlorins via an oxidative intramolecular cycloaddition was observed. An aryl carbon ortho to the meso linkage attacked the β-carbon of an adjacent pyrrole ring, accompanied by 1,2-migration of a pyrrole β-ethyl substituent and a two-electron oxidation of the initially formed macrocycle. The resulting structures are analogous to benzochlorins. The electronic spectra of the metal-free bases are characterized by intense, long-wavelength bands in the visible region. Molecular structures of the chloroferric complexes of the azabenzofluorantheno- and azabenzpyrenoporphyrin macrocycles (derived from fusion of the fluoranthenyl and pyrenyl substituents, respectively) were obtained by X-ray diffraction. The porphyrin moiety in the azabenzofluoranthenoporphyrin adopted a gable structure, with a 22° fold along a diagonal including the pyrrole-ring C4 and C16 α-carbons. By contrast, the azabenzpyrenoporphyrin was virtually planar.

Introduction

Porphyrins and porphinoid compounds offer opportunities for modulation of physicochemical properties by a wide variety of peripheral substituents. Among structures of interest are those in which the porphyrin π-network is connected to an aromatic system or to additional porphyrin systems by linkers. There are as yet no examples of linkers in which a porphyrin meso carbon is bonded directly to an amino nitrogen. This report describes the synthesis and characterization of 5-(*N*-arylamino) and 5-(*N*-arylamido)octaethylporphyrin derivatives with phenyl-, 3-fluoranthenyl-, and 1-pyrenylaryl groups. In developing routes to amino-linked octaethylporphyrin systems, we observed the facile formation of fused azaaryl chlorins from 5-(*N*-arylamino)-octaethylporphyrins via an intramolecular cycloaddition involving attack of an aryl carbon ortho to the meso linkage at the β-carbon of an adjacent pyrrole ring. There are only a few examples of such pyrrole β-to-meso-carbon fused systems. These include several benzochlorins,[1−5] naphthochlorins, naphthoporphyrins,[6−9] and a bischlorin fused along the *bc* and *gh* edges of 1,5-naphthyridine.[10]

Novel porphyrin bases and Zn(II) complexes of potential utility to research on dyes, photodynamic therapy and disinfection, electrooptical properties, and the photosynthetic reaction center are accessible through application of the synthetic routes developed here. Iron complexes are of interest as models for heme adducts derived from peroxidative metabolism of arylamines by hemoglobin and myoglobin.[11−13]

Results

Synthesis and Characterization. Initial efforts to synthesize 5-(*N*-arylamino) derivatives of octaethylporphyrin (OEP) derivatives followed the procedure reported for meso substitution of octaalkyl porphyrins by pyridine and imidazole.[14] In contrast to the more usual electrophilic substitution scheme, these

[†] Department of Environmental Sciences and Engineering.
[‡] Department of Chemistry.

(1) Garca, M.; Vicente, H.; Rezzano, I. N.; Smith, K. M. *Tetrahedron Lett.* **1990**, *31*, 1365−1368.
(2) Mettath, S.; Shibata, M.; Alderfer, J. L.; Senge, M. O.; Smith, K. M.; Rein, R.; Dougherty, T. J.; Pandey, R. J. *Org. Chem.* **1998**, *63*, 1646−1656.
(3) Kosyrev, A. N.; Zheng, G.; Zhu, C.; Dougherty, T. J.; Smith, K. M.; Pandey, R. *Tetrahedron Lett.* **1996**, *36*, 6431−6434.
(4) Boyle, R. W.; Dolphin, D. *J. Chem. Soc., Chem. Commun.* **1994**, 2463−2464.
(5) Barkigia, K. M.; Thompson, M. A.; Fajer, J. *New J. Chem.* **1992**, *16*, 599−607.
(6) Krattinger, B.; Nurco, D. J.; Smith, K. M. *Chem. Commun.* **1998**, 757−758.
(7) Barloy, L.; Dolphin, D.; Dupre, D.; Wijesekera, T. P. *J. Org. Chem*, **1994**, *59*, 7976−7985.
(8) Callot, H. J.; Schaeffer, E.; Cromer, R.; Metz, F. *Tetrahedron* **1990**, *46*, 52553-5262.
(9) Lash, T. D.; Roper, T. J. *Tetrahedron Lett.* **1994**, *35*, 7715−7718.
(10) Johnson, C. K.; Dolphin, D. *Tetrahedron Lett.* **1998**, *39*, 4753−4756.
(11) El-Bayoumy, K. Health Effects Institute Research Report No. 64, Cambridge, MA, 1994.
(12) Ringe, D.; Petsko, G. A.; Kerr, D. E.; Ortiz de Montellano, P. R. *Biochemistry* **1984**, *23*, 2−4.
(13) Everse, J.; Johnson, M. C.; Marini, M. A. *Methods Enzymol.* **1994**, *231*, 547−561.
(14) Smith, K. M.; Barnett, G. H.; Evans, B.; Martynenko, Z. *J. Am. Chem. Soc.* **1979**, *101*, 5953−5961.

10.1021/ic000112r CCC: $19.00
Published on Web 07/12/2000

Scheme 1

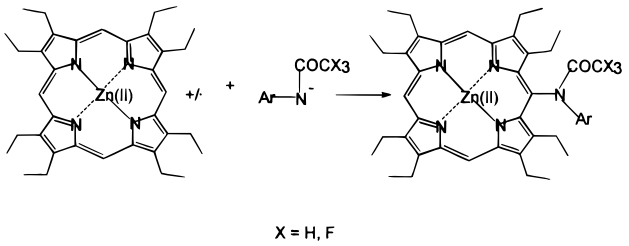

substitutions involve coupling the π-cation radical of meso-unsubstituted Zn(II) or Mg(II) porphyrin complexes with the nitrogen heterocycles. However, when the coupling reaction was performed using primary arylamines, the weaker nucleophilicity of these bases resulted in formation of only trace quantities of products. To enhance the reactivity of the primary arylamines, coupling reactions were repeated with the anionic forms generated from the corresponding *N*-acetamido compounds by treatment with NaH[15] (Scheme 1). Addition of the anionic species generated from acetanilide, 3-acetamidofluoranthene, or 1-acetamidopyrene to Zn(II)OEP$^{\bullet+}$ yielded the expected meso-substituted 5-(*N*-arylacetamido)Zn(II)porphyrin complexes **1a**−**3a** (Table 1), respectively. Extraction of Zn(II) by treatment with HCl-saturated methylene chloride yielded the corresponding 5-(*N*-arylacetamido) porphyrin bases **1b**−**3b** (Table 1). Iron could be inserted into **1b** under mild conditions[16,17] to give ferric complex **1c** (Table 1). However, attempts to insert iron under similar mild conditions into **2b** and **3b** yielded complexes with molecular weights 44 amu lower than required for the target *N*-arylacetamido adducts. These products proved to be ferric complexes of azabenzofluorantheno and azabenzpyreno-fused chlorins described below.

Attempts to obtain *meso*-*N*-arylamino porphyrins from the acetamido derivatives by deacetylation in 3 M methanolic HCl resulted in demetalation. Deacetylation of acetamides **1a**−**3a** did not occur under the mildly reducing conditions used to avoid macrocycle reduction (stirring at ambient temperature with excess NaH in THF). Zinc complexes **1a**−**3a** were recovered unchanged following treatment under a variety of basic conditions. These included refluxing in NH_3-saturated methanol/$CHCl_3$/THF, refluxing in methanol/chloroform with excess triethylamine, or refluxing in methanol/THF with the strong base sodium methoxide. Under more forcing conditions of stirring with excess *n*-butyllithium in THF, the porphyrin ring degraded rapidly even at 0 °C. Consequently, preparation of meso adducts from the more labile trifluoroacetamide derivatives was undertaken (Scheme 1).

Thus, Zn(II) complexes of 5-*N*-phenyl- and *N*-fluoranthenyltrifluoroacetamide adducts, **4** and **5**, respectively (Table 1), were prepared by coupling the anions derived from trifluoroacetanilide and *N*-(3-fluoranthenyl)trifluoroacetamide with Zn(II)OEP$^{\bullet+}$. The Zn(II) complexes of these derivatives were smoothly deacylated by treatment with 20-fold molar excess sodium methoxide in refluxing THF/methanol to the corresponding amino complexes **6a** and **7a** (Table 1). Purification of **7a** also yielded a small quantity of the fused complex **9a** (Figure 1) derived from intramolecular cyclization. Removal of Zn(II) from **6a** gave porphyrin **6b**; however, demetalation of **7a** yielded both the expected porphyrin **7b** (Table 1) and fused porphyrin **9b**

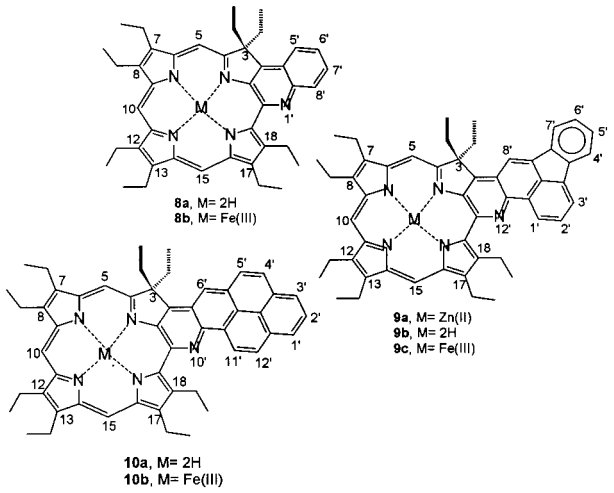

Figure 1. Structural diagrams and numbering schemes for fused systems **8**−**10**.

(Figure 1). Partial metalation of **6b** with ferrous chloride in methanol/chloroform at ambient temperature[16,17] for 10 min yielded the corresponding meso-substituted ferric complex **6c** (Table 1), but even brief refluxing of the metalation reaction mixture yielded fused ferric complex **8b** exclusively. Attempts to insert Fe(II) into **7b** yielded fused ferric complex **9c**. Mass spectra of compounds **8a,b** and **9a**−**9c** showed molecular ions 2 amu less than required for meso adducts. A distinctive feature of the ^{1}H NMR spectra of the diamagnetic compounds in series **8** and **9** was the presence of two methylene resonances shifted to higher field than expected for pyrrole β-ethyl substituents of porphyrins.[2] A similar upfield shift has been reported for the methylene signals of the gem ethyl substituents of the sp^3 β-carbon of the partially saturated pyrrole ring of benzochlorins derived from octaethylporphyrin.[2] The ^{1}H NMR spectra of the paramagnetic ferric complexes **8b** and **9c** showed signals integrating to 12 protons in the range of hyperfine shifts expected for pyrrole β-methylene protons of high-spin ferric porphyrins. Two broad meso proton resonances could be identified over the range −20 to −85 ppm. Both the large upfield shifts and wide range observed for these iron complexes are characteristic of high-spin ferric chlorins.[18] The electronic spectra of all compounds in series **8** and **9** displayed strong bands at long wavelengths, in the range reported for chlorins[19] and benzochlorins.[1,2] Altogether, these data suggested that the macrocycles comprising series **8** and **9** are benzochlorin analogues via formation of a bond between the aryl carbon ortho to the meso amino nitrogen and an adjacent pyrrole β-carbon.

The adduct of Zn(II)OEP$^{\bullet+}$ with 5-*N*-(1-pyrenyl)trifluoroacetamide could not be obtained, but addition of the anion generated from 1-(2,4-dinitrobenzenesulfonamido)pyrene to Zn(II)OEP$^{\bullet+}$ yielded a 1:1 adduct. Because of low solubility and cochromatography with minor byproducts, the Zn(II) complex could not be completely purified. However, after demetalation, a pure compound **10a** could be isolated, which gave ferric complex **10b** on insertion of iron. Spectroscopic characteristics of **10a** and **10b** showed them to be analogues of the corresponding metal-free bases **8a** and **9b** and ferric complexes **8b** and **9c**, respectively. Thus, the 2,4-dinitrobenzenesulfonyl moiety was apparently eliminated during workup, concomitant with intramolecular cyclization to give the pyrene-fused struc-

(15) Bray, B. L.; Mathies, P. H.; Naef, R.; Solas, D. R.; Tidwell, T. T.; Artis, D. R.; Muchowski, J. M. *J. Org. Chem.* **1990**, *55*, 6317−6328.
(16) Jagessar, R. C.; Shang, M.; Scheidt, W. R.; Burns, D. H. *J. Am. Chem. Soc.* **1998**, *120*, 11684−11692.
(17) Borovkov, V.; Lintuluoto, J. M.; Inoue, Y. *Synlett* **1999**, 61−62.
(18) Licoccia, S.; Chatfield, M. J.; La Mar, G. N.; Smith, K. M.; Mansfield, K. E.; Ancerson, R. R. *J. Am. Chem. Soc.* **1989**, *111*, 6087−6093.
(19) Stolzenberg, A. M.; Strauss, S. H.; Holm, R. H. *J. Am. Chem. Soc.* **1981**, *103*, 4763−4778.

Table 1. Structures and Numbering of Meso N-Substituted Porphyrins

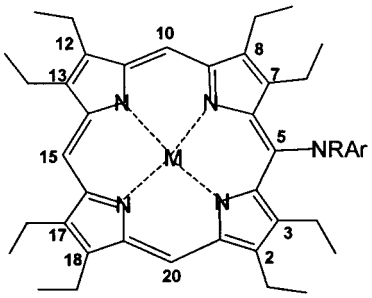

compound	M	R	Ar	compound	M	R	Ar
1a	Zn(II)	-$COCH_3$		**4**	Zn(II)	-$COCF_3$	
1b	2H	-$COCH_3$		**5**	Zn(II)	-$COCF_3$	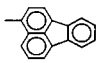
1c	Fe(III)	-$COCH_3$		**6a**	Zn(II)	H	
2a	Zn(II)	-$COCH_3$	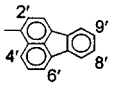	**6b**	2H	H	
2b	2H	-$COCH_3$		**6c**	Fe(III)	H	
3a	Zn(II)	-$COCH_3$		**7a**	Zn(II)	H	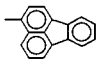
3b	2H	-$COCH_3$		**7b**	2H	H	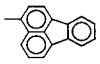

ture. UV−vis and ^{1}H NMR spectra of **9c** and **10b** were identical to the spectra of the products isolated from attempted insertion of iron into *N*-arylacetamido porphyrin bases **2b** and **3b**, respectively. Thus, conditions of insertion of iron into **2b** and **3b** resulted in deacetylation accompanied by intramolecular cyclization to the fused systems. Comparison of UV−vis and ^{1}H NMR spectra of products isolated from attempted insertion of iron into porphyrins **2b** and **3b** established their identities as **9c** and **10b**, respectively. Apparently, redox chemistry accompanying insertion of iron into these porphyrin bases causes deacetylation and cycloaddition with formation of the fused compounds. X-ray structures of ferric complexes **9c** and **10b** confirm the fused chlorin ring structures.

^{1}H NMR. NMR studies of *meso*-dialkylaminoporphyrins with flanking pyrrole β-substituents show that the amino substituents adopt an orthogonal conformation with respect to the porphyrin plane to minimize unfavorable steric interactions.[20] In compounds **1a**,**b**, **2a**,**b**, and **3a**,**b**, steric interactions between the amido nitrogen substituents and the flanking pyrrole β-ethyl groups at C3 and C7 of the porphyrin ring are thus expected to cause the *meso*-*N*-arylacetamido groups to adopt an orthogonal conformation. Steric hindrance can also be expected to slow rotation of the acetamido group around the meso-carbon-to-amido-nitrogen bond as well as rotation around the pyrrole β-methylene bonds of the C3 and C7 ethyl substituents.[20,21] Since the amido substituent bears two different substituents, slow rotation on an NMR time scale will cause the porphyrin plane to lose σ_h symmetry. In **1a**, **2a**, and **3a**, this leaves a C_{2v} plane bisecting the 5,15-meso positions as the only remaining symmetry element. In the spectra of the metal-free bases **1b**, **2b**, and **3b**, two pyrrole N*H* resonances are resolved, indicating that exchange of the pyrrole protons is slow on the NMR time scale. Slow tautomerization along with elimination of the in-plane mirror plane formally removes all symmetry elements. However, the perturbation of C_{2v} symmetry is not sufficient to cause splitting of the meso signals, the most sensitive probes of symmetry. Thus, an approximate C_{2v} plane bisecting the 5,15-meso positions is preserved and three meso proton signals appear as two singlet resonances in a 2:1 ratio in the ^{1}H NMR spectra of the Zn(II) complexes and metal-free bases of all 5-*N*-arylacetamido derivatives. If rotation of the methylene groups is slow on the NMR time scale, the methylene protons of the flanking pyrrole β-ethyl substituents will be diastereotopic. In chloroform-*d*, rapid rotation of the C3 and C7 ethyl groups causes the methylene signals of **1a**,**b** to appear as a four-proton quartet. In methylene-d_2 chloride, however, the signal broadens and the multiplicity increases, indicating incipient resolution of diastereotopic protons (Figure 2).

The upfield position of the methylene multiplet with respect to the envelope representing the remaining β-methylene groups can be can be attributed in part to out-of-plane displacement resulting from steric interactions and in part to rotation of the

(20) Abraham, R. J.; Smith, K. M.; Bobe, F. W.; Minnetian, O. M. *Org. Magn. Reson.* **1984**, *22*, 771−774.

(21) Smith, K. M.; Bobe, F. W.; Minnetian, O. M.; Abraham, R. J. *Tetrahedron* **1984**, *40*, 3263−3272.

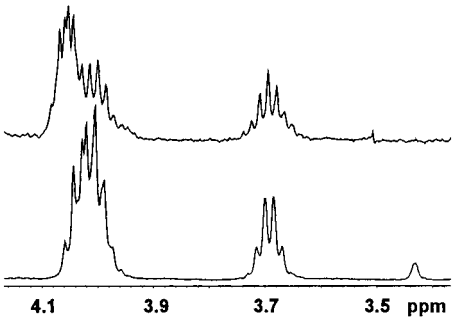

Figure 2. Expansion of methylene region of ^{1}H NMR (500 MHz, ambient temperature) of compound **1b** in (a) chloroform-*d* and (b) methylene-d_2 chloride. Signals between 3.7 and 3.8 ppm belong to the methylene protons of pyrrole β-ethyl substituents at C3 and C7 adjacent to the substituted meso position.

methylene protons into or through the shielding region of the aryl group.[21] In the aromatic region of the ^{1}H NMR spectra of the acetanilide adducts **1a,b**, one- and two-proton triplets are readily assigned to the *p*- and *m*-phenyl protons, respectively. The remaining broadened, deshielded two-proton resonance is assigned to the phenyl *o*-protons. Rotation around the amide nitrogen−phenyl bond would place both *o*-protons in proximity to the deshielding region created by the ring current of the porphyrin and would result in the broadened, averaged peak observed.

The increasing size of the acetamido nitrogen aryl substituent in **2a**,**b** and **3a**,**b** slows the rotation of the flanking methylenes of the C3 and C7 ethyl substituents so that the diastereotopic methylene proton signals are completely resolved as two two-proton multiplets appearing upfield from the envelope containing the remaining methylene resonances. The aryl proton assignments for the *N*-(3-fluoranthenyl)acetamido adducts **2a**,**b** are based on analysis of proton−proton coupling and comparison with ^{1}H NMR spectra of 3-amino-, 3-acetamido-, and 3-trifluoroacetamidofluoranthene.[22] Two upfield pseudotriplets are assigned to H8′ and H9′ of the fluoranthenyl system (Table 1), while the remaining pseudotriplet can be attributed to H5′. The highest and lowest field doublets are assigned to H2′ and H4′, respectively. This assignment is supported by broadening of the H2′ and H4′ resonances observed in the ^{1}H NMR spectrum of the trifluoroacetamido congener **5** (vide infra). H2′ and H4′ are the fluoranthenyl protons closest to the porphyrin periphery and are thus expected to experience the largest variation of ring current effect during rotation about the fluorenyl C3′−amide nitrogen bond. Assignment of the remaining sets of doublets is based on the analysis of coupling constants along with comparison of the NMR spectra with those of other 3-fluoranthenyl compounds.

Strong cross-peaks between the upfield multiplets in the 2D NOESY spectrum of complex **3a** (Figure 3) confirm diastereotopic methylenes on pyrrole β-carbons C3 and C7 as the origin of the upfield methylene multiplets for **3a** as well as for **3b**, **2a**,**b**, and **1a**,**b**. The most upfield of the multiplets is assigned to the diastereotopic protons oriented toward the aryl substituent because these should experience the most pronounced shielding effect from the aryl ring current. In **3a**, the resonances of the methylenes at C2 and C8 are also resolved; the multiplet structure as well as cross-peaks between the two-proton multiplets indicate that these protons are also diastereotopic. The multiplets assigned to the methylene protons or the ethyl

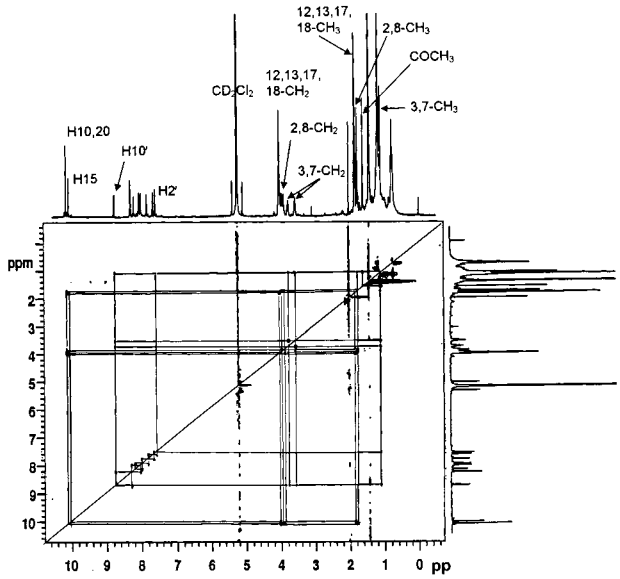

Figure 3. 2D NOESY proton spectrum of compound **3a**. Complete proton assignments are given in the Experimental Section.

substituents at C3 and C7 have a cross-peak with the highest field methyl triplet (1.12 ppm) arising from the ethyl substituents. This triplet may thus be assigned to the C3 and C7 ethyl substituents. A cross-peak between the high-field methyls and the acetyl methyl indicates that these groups are cofacial with respect to the porphyrin plane, confirming a fixed geometry about the C5 *meso*-acetamido nitrogen bond. Cross-peaks are observed between H10′ of pyrene and both diastereotopic C3-(C7) methylene protons as well as the methyl protons of the flanking ethyl substituents. A cross-peak is also observed between the C3(C7) methyl protons and H2′ of pyrene. These interactions can be explained either by rapid rotation of pyrene around the pyrene C1′−acetamido nitrogen bond or by equally populated conformations in which either the C2′−C3′ or the C9′−C10′ edge of pyrene is oriented toward the acetate substituent. Since the rotation of the less bulky phenyl group in **1a** is slowed, rapid rotation of pyrene is unlikely and the latter explanation seems preferable. Consistent with expectation, cross-peaks occur between the symmetry-related meso C10(C20) protons and resonances assigned to the C2(C8) and C12(C18) ethyl protons and between the meso C15 proton and the resonances of the C13(C17) ethyl protons. In the aromatic region of complex **3a**, a pseudotriplet signal at 8.05 ppm can be assigned to H7′ and unambiguous identification of the remaining aromatic protons follows from connectivities established by 2D NOESY NMR.

The porphyrin resonances in the ^{1}H NMR spectrum of the chloroiron(III) complex **1c** appear within hyperfine shift ranges typical of high-spin iron(III) octaalkyl porphyrins.[23,24] Slow rotation around pyrrole β-carbon−methylene carbon bonds superimposed on the asymmetry of unpaired electron spin density distribution arising from the meso amido substituent gives rise to a complex pattern of pyrrole β-methylene resonances. Extremely broad meso resonances appear at −50.2 and −60.7 ppm in a 2:1 ratio, respectively. Two broad signals at 10.2 and 11.3 ppm are tentatively assigned to the phenyl *o*-proton resonances, which are the phenyl protons expected to show the largest contact shift. Resolution of two *o*-proton signals

(22) Ball, L. M.; Stocking, L. M.; Kohan, M. J.; Warren, S. H.; Lewtas, J. *Mutagenesis* **1995**, *10*, 497−504.

(23) La Mar, G. N.; Walker, F. A. In *The Porphyrins*; Dolphin, D., Ed.; Academic Press: New York, 1978; Vol. IVB, pp 61−157.

(24) Goff, H. In *Iron Porphyrins*; Lever, A. B. P., Gray, H. B., Eds.; Addison-Wesley: Reading, MA, 1983; Part I, pp 237−281.

suggests slow rotation about the phenyl−amido nitrogen bond, superimposing rotational broadening upon paramagnetic broadening.

The ^{1}H NMR spectra of the Zn(II) *N*-aryltrifluoracetamido adduct complexes **4** and **5** are similar to the spectra of acetamide analogues. Rotation about the aryl−amide nitrogen bond at an intermediate rate on the NMR time scale results in considerable broadening of the *o*- and *m*-phenyl resonances in the spectrum of **4** and of the H4′ and H2′ fluoranthenyl resonances in the spectrum of **5**.

The ^{1}H NMR spectra of 5-*N*-phenylamino-substituted Zn(II) complex **6a** and porphyrin **6b** are consistent with approximate C_{2v} symmetry, as in the case of the acetamido adducts. The three meso proton signals appear as two singlets with an integral ratio of 2:1. A notable feature of the *o*-proton signals is rotational broadening and a marked shift upfield by ∼2 ppm higher with respect to the *o*-phenyl resonances of acetanilide derivatives **1a,b**. Both rotational broadening and increased shielding may be explained by decreased steric interaction between the flanking pyrrole C3 and C7 β-ethyl substituents and the monosubstituted *meso*-amino group. Rotation of the amino substituent toward a coplanar orientation becomes thermodynamically favorable to allow conjugation between the nitrogen lone pair and the porphyrin frontier π molecular orbitals.[24,25] Some increased conjugation of the amino lone pair is supported by increased shielding of the meso proton resonances compared to those of the acetanilide or trifluoroacetanilide derivatives.[25] Molecular models suggest that rotation of the amino substituent toward the porphyrin plane will position one phenyl *o*-proton over a flanking pyrrole ring, within the shielding region of the porphyrin ring current. Since only a single two-proton *o*-phenyl resonance is observed for **6a** and **6b**, the *o*-positions must be averaged by rotation of the phenyl group around the phenyl−amino nitrogen bond. Steric interaction between the phenyl ring and pyrrole β-ethyl group would be expected to slow rotation, resulting in the observed signal broadening. The two-proton pseudotriplet of the phenyl *m*-protons also shows rotational broadening. The amino proton resonance (7.81 ppm) appears as a sharp singlet as does the signal of the strongly shielded pyrrole NH protons of porphyrin **6b**. The appearance of the methylene resonances of the C3 and C7 β-ethyl substituents as two two-proton diastereotopic signals requires that there be no rotation about the pyrrole C β-methylene bonds.

The porphyrin proton signals of chloroiron(III) complex **6c** appear at shifts expected for a high-spin ferric complex (Figure 4). The methylene signals are spread over the range 37−44 ppm as three sets of broadened singlets representing four methylene protons each and four one-proton singlet resonances. This pattern suggests perturbation of unpaired spin density distribution by the meso substituent superimposed upon approximate C_{2v} symmetry. The pattern also implies rotational averaging of methylene positions of the pyrrole β-C substituents, with the exception of those at C3 and C7, which flank the substituted meso carbon. Percolation of **6c** through $NaHCO_3$ causes no significant change in the methylene pattern, but new resonances develop at −67.5 and −69.4 ppm in the region of the meso proton signals. Percolation of a methylene chloride/methanol solution of **6c** through grade I basic alumina in an attempt to generate an authentic μ-oxodiiron complex[26] yielded a compound with broad methylene resonances between 27 and 33 ppm. The possible significance of these changes along with correlated changes in electronic spectra is discussed below.

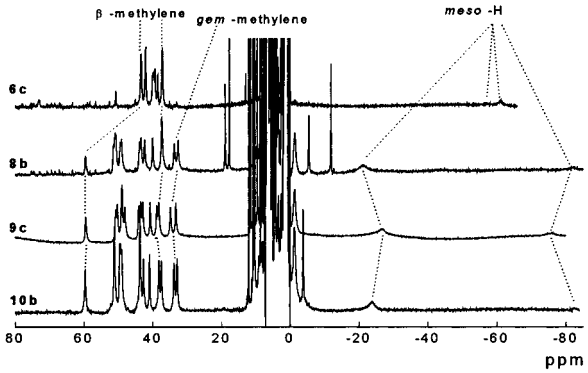

Figure 4. ^{1}H NMR spectra, from top to bottom: complex **6c** (500 MHz, chloroform-*d*); complex **8b** (600 MHz, chloroform-*d*); compound **9c** (500 MHz, chloroform-*d*); complex **10b** (500 MHz, methylene-d_2 chloride). Sharp resonances in the region +20 to −12 ppm are assigned to protons of the fused aromatic moiety. Additional proton assignments are given in the Experimental Section.

The ^{1}H NMR spectra of the Zn(II) complex of the 5-*N*-(3-fluoranthenyl)amino adduct **7a** and the corresponding porphyrin **7b** show one significant change relative to the amido derivatives. The resonance of fluoranthene H2′ experiences a strong shielding effect, shifting upfield to 5.3 ppm in Zn(II) complex **7a** and to 5.6 ppm in porphyrin **7b**. The shielding parallels the behavior of the phenyl *o*-proton signals of **6a** and **6b**, caused by rotation of the monosubstituted amine toward the porphyrin plane to allow conjugation of the amino nitrogen lone pair with the porphyrin frontier π-MOs. Consistent with this picture, the meso proton signals of **7a** and **7b** are less deshielded than those of the amido derivatives. The signals of the meso amino protons of **7a** and **7b** appear as singlets at ∼8.8 ppm.

The ^{1}H NMR spectra of the metal-free chlorin bases are closely similar to each other and show that fusion of the aromatic moiety causes major perturbation of porphyrin electronic structure. The meso resonances of **8a** appear as three widely spaced singlets (7.59, 8.00, 8.73 ppm) and methylene proton resonances of pyrrole β-ethyl substituents as six multiplets ranging from 2.8 to 4.2 ppm (Figure 5).

In addition, the markedly diminished deshielding of the meso protons indicates major disruption of ring current relative to the porphyrin macrocycle, as reported for octaethylbenzochlorin and other benzo-fused chlorin systems.[1−3] Proton assignments were made by 2D NOESY ^{1}H NMR. The shifts of two two-proton methylene multiplets at 2.82 and 3.03 ppm are consistent with gem substituents on sp^3-hybridized C3 of the macrocycle. A strong cross-peak between these signals in the NOESY spectrum confirms this assignment and establishes the diastereotopic character of these protons. Since the C3 ethyl groups are symmetry-related through reflection in the macrocycle plane, each multiplet represents two diastereotopic protons related by this symmetry operation. The signal at 3.03 ppm has a cross-peak with the quinoline doublet at 8.70 ppm. It is therefore assigned to the diastereotopic methylene protons facing the fused ring, while the doublet at 8.70 ppm must arise from quinolino proton H5′ adjacent to the site of fusion at C2 of the heme macrocycle (Figure 1). This assignment is consistent with the expectation that the gem methylene protons facing the fused quinolino system experience a deshielding ring current effect. Identification of H5′ allows connectivity to be established for

(25) Scheer, H.; Katz, J. K. In *Porphyrins and Metalloporphyrins*; Smith, K. M., Ed.; Elsevier Scientific Publishing Co.: Amsterdam, The Netherlands, 1975; pp 426−437.
(26) La Mar, G. N.; Eaton, G. R.; Holm, R. H.; Walker, F. A. *J. Am. Chem. Soc.* **1973**, *95*, 63−75.

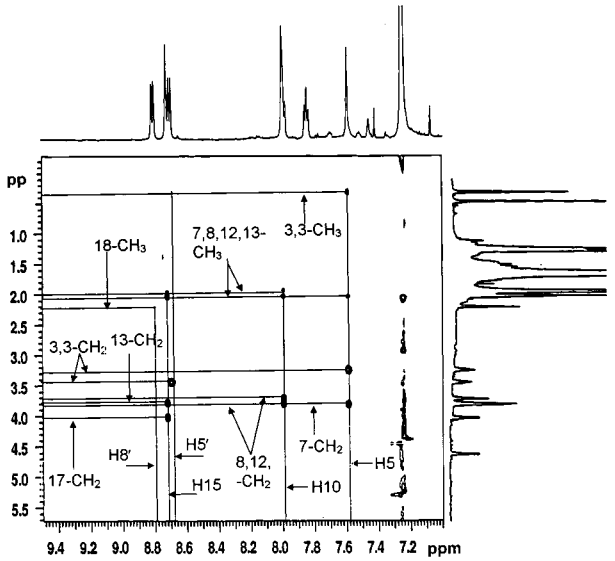

Figure 5. Cross-peaks between the aromatic protons and heme β-ethyl protons in 2D NOESY proton spectrum of compound **8a**.

the quinoline proton resonances. The gem methylene protons facing away from the fused system have a cross-peak with the chlorin meso signal at 7.59 ppm, which is therefore assigned to meso H5. The methylene protons of the C18 pyrrole β-ethyl substituent are situated within a molecular indentation facing the quinolino system and would be expected to experience a deshielding effect. On this basis, the signal at 4.20 ppm is assigned to the C18 methylene group. The methylene resonance at 3.61 ppm has cross-peaks with a signal at 4.20 ppm and the meso singlet at 8.73 ppm, leading to the assignment of the signal at 3.61 ppm to the C17 methylene group and of the meso resonance to H15. The remaining quinolino doublet must belong to H8′. From NOESY cross-peaks the pseudotriplets at 7.84 and ~8 ppm are assigned to H6′ and H7′, respectively. An ambiguity in proton assignments involves the methylene groups at C8 and C12, which have cross-peaks with meso H10 but with no other signals and thus cannot be distinguished. Proton assignments for **9b** and **10a** (2D NOESY spectra and connectivities presented in Supporting Information) were made using a similar approach and are given for each compound in the Experimental Section.

The hyperfine shifts of the iron complexes of the fused porphyrins are in accord with high-spin ferric complexes, with superposition of large asymmetry in the distribution of unpaired electron spin density at porphyrin ring carbons induced by the fused aryl rings[27] and concomitant saturation of one pyrrole carbon.[18] These effects are evident from comparison of the ^{1}H NMR spectra of the ferric complexes in Figure 5. In general, meso proton resonances of high-spin ferric chlorins are expected to be extremely broad and to experience upfield hyperfine shifts, with signals from inequivalent meso protons spread over a wide range.[18,28] Ferric complexes **8b**, **9c**, and **10b** all show two resonances at about −80 and about −20 ppm. While extreme broadening and poor resolution rule out a definitive conclusion that the peaks represent one-proton signals, absence of a symmetry element leads to the expectation of a third undetected meso resonance, most likely obscured within the envelope of diamagnetic signals around 0 ppm. The low-field region of the three ferric complexes are qualitatively similar to that reported for the chloroferric complex of octaethyl chlorin.[28] In the spectrum of complex **8b** (Figure 4), 12 signals appearing between 37 and 60 ppm are thus assigned to the methylene protons of pyrrole β-ethyl substituents. Four additional one-proton singlets at 33.8, 32.6, 10.2, and 8.8 ppm are paramagnetically broadened and on this basis can be assigned to the gem methylene protons. One-proton singlets at 18.9, 17.8, −5.5, and −11.9 ppm show considerably smaller paramagnetic interaction, consistent with expectations for the quinolino protons. The methyl resonances of the pyrrole β-ethyl substituents appear as poorly resolved, highly broadened resonances between 5 and 7 ppm. A broad three-proton resonance at −1.4 ppm is tentatively assigned to the methyl group of a gem ethyl substituent from analogy to the crystal structures of ferric complexes **9c** and **10b**, in which a methyl group is situated in the shielding region created by the porphyrin ring current.

The ^{1}H NMR spectrum of ferric complex **9c** (Figure 4), like that of the quinolino-fused ferric complex **8b**, is consistent with a high-spin ferric complex having a highly asymmetric distribution of unpaired electron spin density. Resonances of 12 pyrrole β-methylene protons extend from 37 to 59 ppm. Four broadened resonances at 34.8, 33.3, 10.7, and 9.5 ppm are assigned to the methylene protons of the gem ethyl substituents. The methyl signals of the pyrrole β-ethyl groups are included within an envelope spanning 6.7−5.9 ppm. A highly shielded, paramagnetically broadened three-proton resonance at −1.3 ppm is tentatively assigned to the methyl group of a gem ethyl on the basis of the crystal structure, which shows one methyl situated within the shielding region of the macrocycle ring current. One-proton resonances with relatively little paramagnetic broadening are assigned to the aryl protons of the fused azabenzofluoranthene.

In the ^{1}H NMR spectrum of ferric complex **10b** (Figure 4), like that of **9c**, signals of 12 pyrrole β-methylene protons appear over the range 37−60 ppm. Paramagnetically broadened one-proton resonances at 33.8, 32.9, 9.1, and 8.7 ppm are assigned to methylene protons of the gem ethyl substituents. The methyl signals of the pyrrole β-ethyl substituents appear within an envelope of broad absorbances ranging from 7.3 to 3.1 ppm. As for **9c**, a broadened three-proton resonance at −1.3 ppm is assigned to the methyl signal of a gem ethyl group. Signals with smaller paramagnetic interactions must arise from the fused azabenzpyrene protons.

Electronic Spectra. The porphyrin chromophore of the meso acetamido adducts shows no significant perturbation relative to that of octaalkyl porphyrin compounds. The spectra of Zn(II) complexes **1a**, **2a**, and **3a** do differ slightly from the spectrum of unmodified Zn(II)OEP by an increase in the $Q_{1,0}/Q_{0,0}$ band intensity ratio.[29] In the electronic spectra of the fluoranthene and pyrene derivatives **2a**,**b** and **3a**,**b**, bands characteristic of the aromatic chromophores are resolved.[30] The limited interaction between the π-systems indicates that the amido group is oriented perpendicular to the porphyrin plane, preventing conjugation of the nonbonding amido nitrogen electrons with the porphyrin π-frontier MOs. An orthogonal orientation of the acetamido group is also indicated in the electronic spectrum of ferric complex **1c**, which is qualitatively similar to that of the chloroferric complex of octaethylporphyrin,

(27) Wojaczynski, J.; Latos-Grazynski, L.; Glowiak, T. *Inorg. Chem.* **1997**, *36*, 6299−6306.
(28) Pawlik, M. J.; Miller, P. K.; Sullivan, E. P., Jr.; Levstik, M. A.; Almond, D. A.; Strauss, S. H. *J. Am. Chem. Soc.* **1988**, *110*, 3007−3012.
(29) Gouterman, M. In *The Prophyrins*; Dolphin, D., Ed.; Academic Press: New York, 1978; Vol. I, pp 1−166.
(30) Clar, E. *Polycyclic Hydrocarbons*; Academic Press: New York, 1964; Vol. 2, pp 110−126, 295−302.

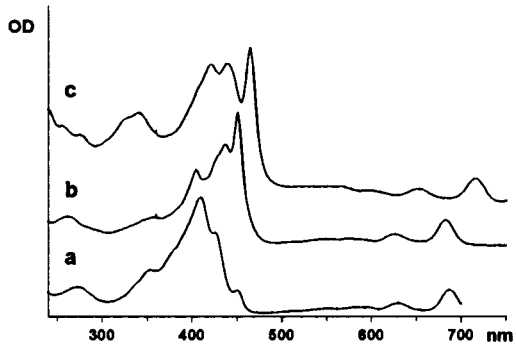

Figure 6. Electronic spectra (methanol, ambient temperature) of (a) **8a**, (b) **9b**, and (c) **10a**.

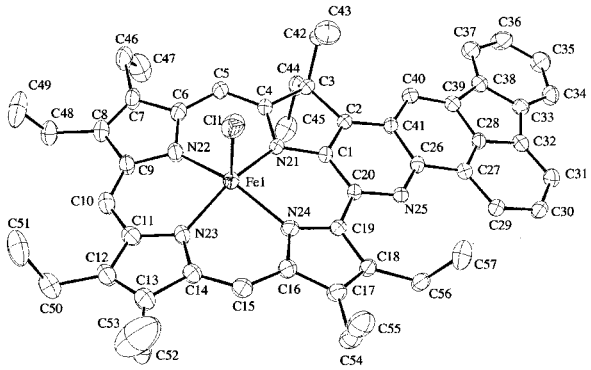

Figure 7. ORTEP drawing of complex **9c** with numbering scheme used in solving the structure.

but slightly red-shifted, with the B band at 396 nm and visible bands at 500 and 625 nm. The electronic spectra of Zn(II) *N*-aryltrifluoracetamido compounds **4** and **5** are similar to the spectra of the acetamide analogues.

The electronic spectra of *meso*-anilinyl-substituted porphyrin **6b** and Zn(II) complex **6a** appear qualitatively similar to those of the corresponding unmodified OEP compounds. Absorption maxima are slightly red-shifted relative to the absorption maxima of the acetanilides **1a**,**b** and exhibit a 5−10 nm global red shift relative to those of octaethylporphyrin and its Zn(II) complex, respectively. Some conjugation of the amino nitrogen lone pair with the porphyrin ring in **6a**,**b** is thus indicated, consistent with NMR data showing rotation of the *N*-phenyl substituent toward the porphyrin plane. As is the case for Zn(II) complexes **1a**, **2a**, and **3a**, the ratio of the visible bands $Q_{1,0}/Q_{0,0}$ of Zn(II) complex **6b** is reversed in intensity relative to OEPZn(II). The chloroiron(III) complex generated by treatment of ferric *meso*-*N*-phenylaminoporphyrin **6c** with HCl has an electronic spectrum very similar to that of the chloroiron(III) complex of octaethylporphyrin. Following percolation of **6c** through $NaHCO_3$, the electronic spectrum is characterized by splitting of the B band, with maxima appearing at 354 and 404 nm and a broad visible band at 563 nm. These changes are concomitant with changes in the NMR spectrum described above. On percolation of a methylene chloride/methanol solution of **6c** through activity grade I basic alumina, the electronic spectrum is characterized by B band splitting with maxima at 354 and 404 nm and a visible band at 580 nm.

The electronic spectra of the *meso*-*N*-(3-fluoranthenyl)amino adduct of octaethylporphyrin **7b** and the Zn(II) complex **7a** are similar to those of the respective *N*-phenyl homologues, showing effects of conjugation of the aryl π-system with the porphyrin ring by global red shifts of both B and visible bands. Bands in the UV region are perturbed relative to both fluoranthenyl and 3-aminofluoranthenyl chromophores. In accord with the NMR data, these changes in the electronic spectra suggest some conjugation of the nitrogen lone pair with the porphyrin π-system.

The electronic spectra of metal-free fused bases (Figure 6) are qualitatively similar to spectra reported for octaalkyl benzochlorins, characterized by fine structure in the B bands and intense, strongly red-shifted Q bands.[1,2] In the spectrum of quinolinochlorin **8a**, shoulders on both the short and long wavelength edges of the B band are resolved. The strongly enhanced, red-shifted Q band appears at 687 nm.

In the electronic spectrum of the metal-free base **9b** multiple B bands at 439 and 455 nm are observed (Figure 7), with a Q band at 686 nm. The electronic spectrum of Zn(II) complex **9a** features multiple B bands at 447 and 471 nm strongly red-shifted relative to the metal-free base. An intense Q band occurs at the exceptionally long wavelength of 725 nm. Similar marked global red shifts in the electronic spectra of Zn(II) complexes relative to those of metal-free bases have been observed for benzochlorin derivatives.[2] The electronic spectrum of the fused azabenzpyrene system **10a** is qualitatively similar to that of chlorin base **9b**, but bands in both B band and visible regions are red-shifted relative to **9b**. Multiple λ_{max} appear in the B band region at 421, 439, and 465 nm, and an intense visible band appears at 716 nm.

While Zn(II) and Ni(II) derivatives of fused benzo- and naphthooctaalkylchlorins have been reported, no reports of analogous iron complexes are available for direct comparison with isostructural models. However, the salient features of the chloroferric complexes of the fused systems in this report are in general conformity with expectations for ferric chlorins, having visible bands strongly red-shifted relative to the corresponding porphyrin absorbances.[19] The identifying features of the electronic spectrum of **8b** are a B band at 414 nm with the most prominent visible band at 686 nm. The electronic spectrum of ferric complex **9c** consists of a red-shifted B band at 438 nm and a broad band at 675 nm in the visible region. The B band of the ferric complex **10b** appears at 437 nm, with the visible region displaying broad, poorly resolved low-intensity bands at 642 and 702 nm.

Crystal Structures. The molecular structures of ferric complexes **9c** and **10b** were determined by X-ray crystallography. Crystallographic data are summarized in Table 2.

Complex **9c** crystallizes in space group $P2_1/c$, which imposes no particular symmetry on the molecular structure of **9c**. In the unit cell, molecules of **9c** are associated as face-to-face pairs, related by an inversion center, with the axial chloro ligands coordinated to iron on the outside faces. Figure 7 is an ORTEP drawing of a single molecule of **9c** showing the atom numbering scheme used in solution of the structure.

Each macrocycle is folded along a line passing through C4 and C16 so that the molecule has a distinct "gable" roof conformation with an angle of 22.28(7)° between the mean dihedral planes of the gable roof. The macrocycles are slipped so that the planes comprising the long roof overlap and are parallel. The associated gables thus nest in a complementary fashion (Figure 8). Minimum distances between overlapping planes of nested molecules are 3.35 Å between C29 and C20 of a facing molecule and 3.46 Å between C15 and C34 of a facing molecule. These separations are indicative of $\pi-\pi$ interactions, primarily between the fluoranthene ring and the quadrant of the opposing chlorin-containing pyrrole ring C16−C19−N24 between meso positions C15 and C20. In this regard stacking differs from that found for the metal-free base of

Table 2. Summary of Crystallographic Data

	9c	**10b**
formula	$C_{53}H_{52}Cl_4FeN_5$	$C_{54}H_{53}Cl_7FeN_5$
mol wt	956.68	1076.06
cryst syst	monoclinic	monoclinic
a (Å)	13.1268(11)	9.8832(5)
b (Å)	14.9253(13)	22.0438(11)
c (Å)	23.9850(20)	12.3407(6)
β (deg)	95.990(2)	108.856(1)
V (Å^3)	4673.5(7)	2544.30(22)
Z	4	2
D_{calc} (Mg m^3)	1.360	1.405
λ (Å)	0.710 73	0.710 73
μ (cm^{-1})	5.9	7.1
space group	$P2_1/c$	$P2_1$
diffractometer	Bruker SMART 1K	Bruker SMART 1K
cryst size (mm)	0.20 × 0.20 × 0.10	0.20 × 0.20 × 0.05
temp (°C)	−173	−173
radiation	Mo Kα	Mo Kα
monochromator	graphite	graphite
mode	ω	ω
scan width (deg)	0.3	0.3
octants	$\pm h \pm k \pm l$	$\pm h \pm k \pm l$
2θ (min/max) (deg)	5.0/50.0	5.0/50.0
no. data collected	91 177	17 243
no. unique data	8284	8718
no. data with $I > 2.5\sigma(I)$	5013	5143
no. variables	563	603
$R(F)$	0.051 (0.084)	0.071 (0.128)
$R_w(F)$	0.057 (0.060)	0.074 (0.079)
largest peak in final difference map (e Å^{-3})	0.690	0.490
GOF	1.3951	1.9166

octaethylbenzochlorin in which neither the pyrrole nor fused benzo rings overlap directly.

Figure 9 shows the deviation of atoms from the mean plane defined by the 24-atom chlorin core in units of 0.01 Å. The general structural features of **9c** are similar to those expected for a high-spin ferric heme complex, with iron displaced 0.5076(11) Å out of the mean plane of the 24 core atoms and 0.4423(19) Å out of the mean plane of the four coordinated nitrogens toward the chloro ligand situated at 2.2245(14) Å from iron. There are two long and two short Fe−$N_{pyrrole}$ distances. The long bonds are between iron and the nitrogen of the fused, partially saturated pyrrole and between iron and the nitrogen of the pyrrole adjacent to the fused meso position (Table 1). The pyrrole rings are planar, but displacements of the pyrrole β-carbons with respect to the mean plane of the 24-atom chlorin core show a slight twist around the Fe−$N_{pyrrole}$ bonds (Figure

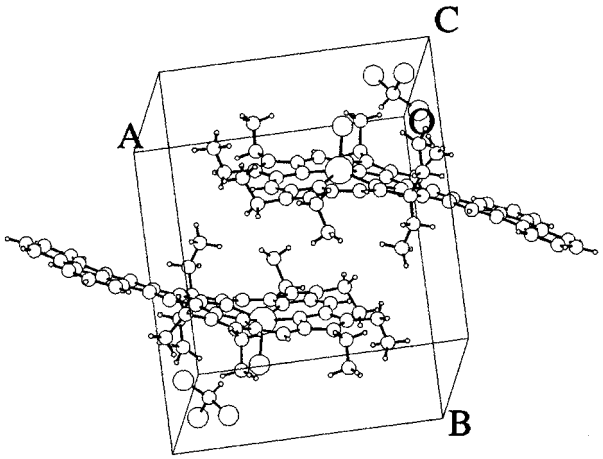

Figure 8. Unit cell of **9c** with two symmetry-related molecules removed for clear illustration of nesting.

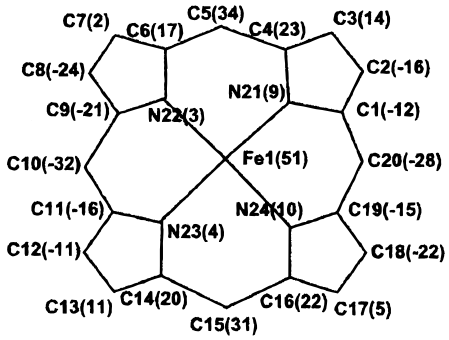

Figure 9. Displacement of the 24 porphyrin core atoms of **9c** from mean plane of the core in units of 0.01 Å.

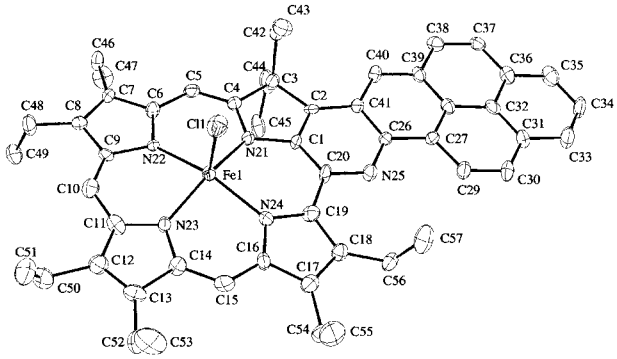

Figure 10. ORTEP drawing of complex **10b** with numbering scheme used in solving the structure.

10). The C2−C3 and C3−C4 bonds of the partially saturated pyrrole have, as expected, predominantly single bond character (Table 2), and the C2−C3−C4 bond angle of 100° is smaller than for a pyrrole ring. This distortion is accompanied by a slight spreading of the internal angles at pyrrole N21 and α-C (C1, C4). The six-membered heterocyclic ring bridging the fluoranthene system and porphyrin periphery is fully aromatic. One internal angle C2−C41−C26 (at the junction of the partially saturated pyrrole ring and aromatic system) is compressed to 114°. Thus, the entire macrocycle framework forms an extended, conjugated π-system with the exception of gem-substituted, sp^3-hybridized C3.

Complex **10b** crystallizes in the space group $P2_1$, which imposes no symmetry on the molecular structure of **10b**. In the absence of a symmetry element in the molecular structure, the space group requires that the crystals contain single enantiomers and therefore that the crystals be chiral. Figure 10 is an ORTEP drawing showing the numbering scheme used in solving the structure. In contrast to the structure **9c**, the entire macrocycle of **10b** is virtually planar, with only a very small doming (Figure 11). The only overlap between symmetry-related molecules is between pyrene C37−C38 and pyrrole C7−C8 peripheral bonds (Figure 12).

The shortest intermolecular distances are C37−C7 = 3.49 Å and C38−C8 = 3.38 Å, indicating that overlap involves $\pi-\pi$ interaction between these bonds. As for complex **9c**, other structural features are consistent with a high-spin ferric heme complex. Iron is displaced 0.5168(24) Å from the mean plane of the 24 core atoms and 0.436(4) Å from the mean plane of the four pyrrole nitrogens toward the chloro ligand, which is situated at 2.22430(24) Å from iron. As for **9c**, iron is coordinated to the macrocycle by two long and two short bonds, the long distances being to the nitrogen of the partially saturated pyrrole and to the nitrogen of the pyrrole ring adjacent to the fused meso carbon (Table 3). The C2−C3 and C3−C4 bonds

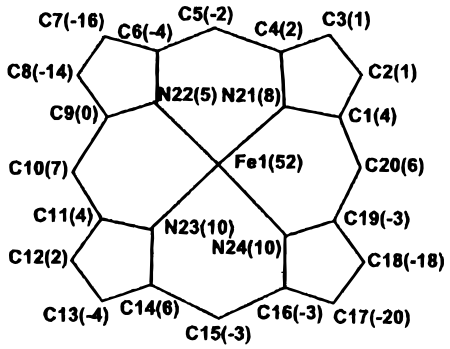

Figure 11. Displacement of the 24 porphyrin core atoms of **10b** from mean plane of the core in units of 0.01 Å.

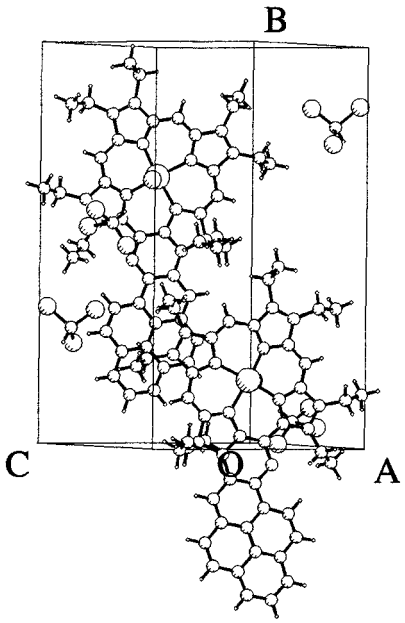

Figure 12. Packing of molecules of **10b** in the unit cell.

of the partially saturated pyrrole have predominantly single bond character (Table 3), with the C2−C3−C4 bond compressed to 103°. As in the case of the fused fluoranthene system, the six-membered heterocyclic ring bridging the porphyrin and aromatic moieties is aromatic so that the entire macrocyclic framework, with the exception of gem-substituted sp^3-hybridized C3, is a delocalized π-system.

Discussion

The modified procedure for nucleophilic addition of amide nitrogen to the porphyrin meso position provides accessibility to a wide variety of *meso*-arylamido- and arylamino-substituted porphyrins. NMR data acquired in characterizing the compounds in series **1**−**7** can be interpreted according to studies on meso mono- and disubstituted aminoporphyrins.[20,21] These reports demonstrate that the orientation of the amino substituents with respect to the porphyrin plane is a function of steric interactions between the amino substituents and flanking pyrrole β-substituents. Thus, *meso*-arylaminoporphyrins **6a**−**c** and **7a**,**b** show a dramatic shielding of aryl protons ortho to the amino nitrogen, resulting from rotation of the amino substituent toward the plane of the porphyrin and into the shielding region of the porphyrin ring current. Consistent with this change in orientation, the meso protons are less deshielded in the *meso*-*N*-arylamino-substituted compounds than in the *meso*-*N*-arylamido derivatives. The appearance of diastereotopic methylene signals confirms the

Table 3. Selected Bond Distances (Å) and Bond Angles (deg) with Estimated Standard Deviations in Parentheses

	9c	**10b**
Fe(1)−Cl(1)	2.2250(14)	2.2430(24)
Fe(1)−N(21)	2.058(3)	2.078(7)
Fe(1)−N(22)	2.048(3)	2.054(7)
Fe(1)−N(23)	2.033(3)	2.024(7)
Fe(1)−N(24)	2.067(3)	2.089(7)
C(2)−C(3)	1.512(5)	1.500(13)
Cl(1)−Fe(1)−N(21)	100.73(10)	100.28(22)
Cl(1)−Fe(1)−N(22)	101.39(11)	102.21(21)
Cl(1)−Fe(1)−N(23)	104.35(11)	103.90(22)
Cl(1)−Fe(1)−N(24)	103.25(11)	102.40(23)
N(21)−Fe(1)−N(22)	86.71(13)	86.3(3)
N(21)−Fe(1)−N(24)	86.40(12)	86.4(3)
N(22)−Fe(1)−N(23)	86.91(13)	86.1(3)
N(23)−Fe(1)−N(24)	89.32(13)	90.9(3)
C(4)−C(5)−C(6)	126.0(4)	127.9(9)
C(5)−C(6)−C(7)	125.2(4)	124.3(9)
C(9)−C(10)−C(11)	125.8(4)	128.0(10)
C(14)−C(15)−C(16)	128.4(4)	126.3(9)
C(1)−C(20)−C(19)	124.0(4)	124.8(9)

importance of steric interactions between the C3 and C7 pyrrole β-ethyl groups and the amido/amino aryl substituents in determining amino substituent conformation. On the basis of the published correlation between the degree of conjugation of the meso nitrogen lone pair and the level of deshielding of the remaining meso protons,[25] none of the compounds described here, including aminoporphyrins **6a**−**c** and **7a**,**b**, exhibit strong conjugation. Support for this conclusion is evident in the relatively small extent to which the electronic spectra of porphyrins **6b** and **7b** are perturbed when compared to the spectra of octaethylporphyrin and the *meso*-amido-substituted porphyrins. Similarly, comparison of the electronic spectra of zinc(II) complexes **6a** and **7a** with the zinc(II) complexes of octaethylporphyrin and the *meso*-amido- or trifluoroacetamidoporphyrins indicates relatively little effect of conjugation. Nevertheless, the orientational effects reported here suggest an approach to modulating conjugation of the meso nitrogen lone pair with the porphyrin π-system by engineering the extent of substituent interactions. Thus, it should be possible to achieve control of communication between the porphyrin and appended *meso*-amido/amino substituents, which should be useful in exploring models of biological relevance to charge transfer.

Of the amino complexes, iron could be inserted only into the *meso*-*N*-phenylamino derivative without causing intramolecular cycloaddition to form a fused system. Treatment of the ferric *meso*-*N*-phenylaminoporphyrin **6c** with HCl leaves ambiguity with regard to the protonation state of the meso amino nitrogen. Formation of an ammonium ion would block conjugation of the lone pair of the amino nitrogen with the porphyrin. As a result, the electronic spectrum would be expected to show little perturbation relative to that of the chloroiron complex of octaethylporphyrin, as observed. However, in the absence of a crystal structure, it is not possible to distinguish this situation from one in which the amino substituent has adopted an orthogonal orientation. The tendency of the monosubstituted arylamine to assume a coplanar orientation in the ferric complex cannot be assessed on the basis of published studies, which include only porphyrin bases and the corresponding dications generated with trifluoroacetic acid. Percolation of **6c** through $NaHCO_3$ will ensure the presence of the meso amino substituent in the neutral form. However, the nature of the axial ligand is uncertain. Complex **6c** was treated with activity grade I basic alumina in an attempt to generate a μ-oxodiiron derivative for purposes of comparison. This treatment yielded a compound

Scheme 2

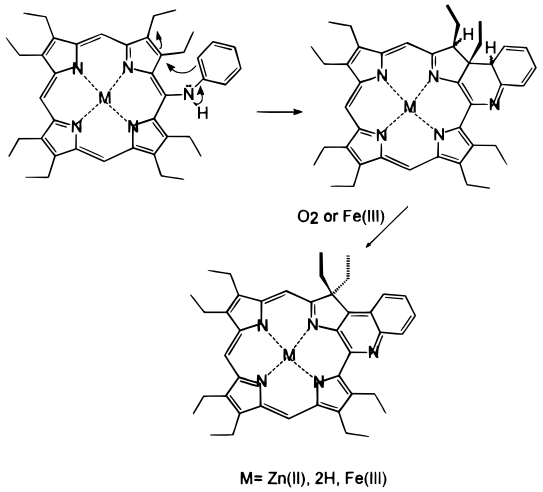

with pyrrole β-methylene signals having hyperfine shifts between those of a high-spin ferric monomer and μ-oxodiiron complex[26] and an electronic spectrum similar to that of bicarbonate-treated **6c**. While no definitive structural assignment is possible, these data could be explained by formation of a hydroxo complex with bicarbonate and a hexacoordinate intermediate-spin[31] or spin-admixed complex ($S = {}^3/_2, {}^5/_2$)[32] on treatment with basic alumina in methanol/methylene chloride.

The formation of fused systems **8**−**10** is an unusual reaction. The apparent facility of this reaction may stem from rotation of the arylamino substituents toward the porphyrin plane. This orientation brings the aromatic carbons ortho to the meso *N*-aryl substituent into proximity with an adjacent pyrrole β-carbon, which likely facilitates the cycloaddition reaction. A possible mechanism, summarized in Scheme 1, is nucleophilic attack of the imino tautomer of the aryl substituent, which places electron density on an ortho position, at the adjacent pyrrole β-carbon followed by oxidation. This type of fused azaaromatic system is unique. Bond distances in the crystal structures of **9c** and **10b** indicate that the entire π-framework is appropriately treated as one system. This picture is supported by the ^{1}H NMR spectra where proton signals assignable to the fused aromatic systems show hyperfine shifts. The electronic spectra of the azaarene-fused chlorins, both as metal-free bases and metal complexes, are also perturbed, having strongly red-shifted bands compared to octaethyl chlorins. Of interest is the intense band in the visible spectrum of the metal-free bases, which appears >80 nm to the red of the corresponding band of octaethylchlorin and about 20 nm to the red of the corresponding band of octaethylbenzochlorin. Because of the intense, long wavelength absorbance, benzochlorins have been investigated as potential agents for use in photodynamic therapy.[2,33] In addition to extending the visible bands further into the red portion of the electronic spectrum, fused systems, exemplified by compounds such as **8**−**10**, offer potential flexibility in designing physical properties through use of a variety of arenes or peripherally substituted arenes. The crystal structures of iron complexes **9c** and **10b** indicate that fusion of the aromatic systems to the porphyrin periphery and concomitant delocalization of macrocycle electron density result in weakening of the two Fe−N bonds nearest the site of fusion. The effect is more pronounced in the fused pyrene derivative and probably reflects the greater aromaticity of the pyrene structure inferred from the relative enthalpies of formation, $\Delta H°_{f,298} = 53.7$ kcal mol^{-1} for pyrene[34] and $\Delta H°_{f,298} = 69.2$ kcal mol^{-1} for fluoranthene.[35,36]

Experimental Section

General Information. Solvents were purchased commercially (Fisher). Methylene chloride and tetrahydrofuran were distilled from NaH prior to use. Other solvents were used as received. Acetanilide and 1-acetamidopyrene were purchased commercially (Aldrich). 3-Acetamidofluoranthene was synthesized according to a published procedure.[22] Trifluoroacetanilide, 3-trifluoroacetamidofluoranthene, and 1-trifluoracetamidopyrene were obtained in quantitative yields by refluxing the appropriate arylamine (Aldrich) in methylene chloride with trifluoroacetic anhydride, washing the cooled solution twice× with water, and then drying the organic layer over sodium sulfate and removing solvent under reduced pressure.

NMR spectra were recorded either at 500 MHz on a Varian 500 INOVA 500 or at 600 MHz on a Varian INOVA 600. Exact mass measurements and low-resolution mass spectrometric scans were obtained by FAB on a VG70 250SEQ operating in a positive ion mode using *p*-nitrobenzyl alcohol as a matrix. UV−vis spectra were obtained (215−800 nm) on a Milton Roy Spectronic 1201 spectrophotometer.

Crystallization. Crystals of complexes **9c** and **10b** suitable for structural determination by X-ray crystallography were obtained by slow diffusion of hexane into chloroform solutions of the complexes.

X-ray Experimental Section. Small, well-shaped crystals of **9a** and **10b** were attached to the tip of a glass fiber with a small amount of oil and then mounted in the cold stream of a Bruker SMART 1K diffractometer. Initial cell dimensions and orientation matrices were determined and the frames used to evaluate the quality of the crystals. A full sphere of intensity data was then collected with the CCD set to a maximum 2θ of 50°. The Bruker routine SAINT was used to integrate the frames and produce a set of intensities, which were corrected for absorption effects using SADABS. All subsequent computations were performed with the NRCVAX suite of programs[37] using scattering factors taken from ref 38.

The structures were solved using direct methods to locate the non-hydrogen atoms. After several cycles of least-squares refinement the hydrogen atoms were inserted in computed positions and included in the final least-squares cycles using a riding model. Final difference syntheses showed no significant features. The experimental data are summarized in Table 2.

General Procedure: 5-(*N*-Aryltrifluoroacetamido)-2,3,7,8,12,13,17,18-octaethylporphyrinatozinc(II). The trifluoroacetamido arene (0.5 mmol) in 10 mL of THF is stirred with NaH (0.75 mmol) under argon for 15 min. Under argon pressure, the clear solution is added by cannula to a solution of zinc(II) octaethylporphyrin π-cation radical generated in situ by treating zinc(II) octaethylporphyrin (0.05 mmol) in 13 mL of THF with tris(*p*-bromophenyl)aminium hexachloroantimonate (0.1 mmol) in 10 mL of methylene chloride for 5 min. The resulting purple solution is stirred for 3 h under argon and the solvent removed under reduced pressure. The remaining solid is chromatographed on silica eluted with hexane/methylene chloride, 1:1. Unreacted zinc octaethylporphyrin is eluted first followed by the product.

General Procedure: 5-Arylamino-2,3,7,8,12,13,17,18-octaethylporphyrinatozinc (II). The 5-(*N*-aryltrifluoroacetamido)porphyrin complex synthesized above (1 mmol) in methanol/THF, 1:1, was refluxed with sodium methoxide (20 mmol) under argon for 1 h. The

(31) Dolphin, D. H.; Sams, J. R.; Tsin, T. B. *Inorg. Chem.* **1977**, *16*, 711−713.
(32) Cheng, B.; Safo, M. K.; Orosz, R. D.; Reed, C. A.; Debrunner, P. G.; Scheidt, W. R. *Inorg. Chem.* **1994**, *33*, 1319−1324.
(33) Morgan, A. R.; Skalkos, D.; Maguire, G.; Rampersaud, A.; Garbo, G.; Keck, R.; Selman, S. H. *Photochem. Photobiol.* **1992**, *55*, 133−136.
(34) Smith, N. K.; Stewart, R. C.; Osborn, A. G.; Scott, D. W. *J. Chem. Thermodyn.* **1980**, *12*, 919−926.
(35) Ling, Y.; Lifshitz, C. *J. Phys. Chem.* **1995**, *99*, 11074−11080.
(36) Boyd, R. H.; Christensen, R. L.; Pua, R. *J. Am. Chem. Soc.* **1965**, *87*, 3554−3559.
(37) Gabe, E. J.; Le Page, Y.; Charland, J.-P.; Lee, F. L.; White, P. S. *J. Appl. Crystallog.* **1989**, *22*, 384−387.
(38) *International Tables for X-ray Crystallography*; The Kynoch Press: Birmingham, England, 1974; Vol IV.

solvents were removed under reduced pressure and the residue taken up in methylene chloride and washed twice× with equal volumes of water. The organic layer was dried over sodium sulfate and evaporated. The residue was filtered through silica with methylene chloride eluant. The material recovered from the filtrate was purified by TLC on a silica plate (20 cm × 20 cm × 1000 μm) eluted with hexane/methylene chloride, 1:1. Yields are calculated based on Zn(II)OEP starting complex.

a. 5-*N*-Phenylacetamido-2,3,7,8,12,13,17,18-octaethylporphyrinatozinc(II) (1a). Purified **1a** was isolated in 50% yield. UV−vis (MeOH, λ_{max}, nm ($\epsilon \times 10^{-3}$)): 242 (14.26), 337 (16.93), 408 (92.71), 543 (11.42), 582 (10.55). HRMS (FAB$^+$) *m*/*z* calcd for $C_{44}C_{51}N_5O^{64}Zn$ [M$^+$]: 729.3385. Found: 729.3517. LRMS (FAB$^+$), *m*/*z* (rel intensity): 734 (26), 733 (51), 732 (50), 731 (74), 730 (68), 729 (100) [M$^+$], 690 (13), 689 (14), 688 (16), 687 (16), 686 (20). ^{1}H NMR (500 MHz, methylene-d_2 chloride): δ 10.14 (s, 2H, H10, H20), 10.10 (s, 1H, H15), 7.69 (bs, 2H, phenyl *o*-H), 7.05 (pseudo t, 2H, phenyl *m*-H, $J_{ave} = 8.0$ Hz), 6.92 (t, 1H, phenyl *p*-H, $J = 7.3$ Hz), 3.96−4.08 (m, 12H, 2-, 8-, 12-, 13-, 17-, 18-β-CH_2CH$_3$), 3.63−3.73 (m, 4H, 3-,7-β-CH_2CH$_3$), 1.83, 1.86 (overlapping t, 18H, 2-, 8-, 12-, 13-, 17-, 18-β-CH$_2$CH_3, $J = 7.6$ Hz), 1.56 (s, 3H, acetyl), 1.13 (t, 6H, 3-,7-β-CH$_2$CH_3; $J = 7.6$ Hz).

b. 5-(*N*-3-Fluoranthenyl)acetamido-2,3,7,8,12,13,17,18-octaethylporphyrinatozinc(II) (2a). The product demetalated during initial chromatography and was isolated as the metal-free base **2b** in 35% yield based on OEP. Zn(II) was inserted by refluxing for 5 min in hexane/methylene chloride, 1:1, with 20-fold excess ZnOAc. Purified **2a** was obtained in 90% yield based on **2b**. UV−vis (MeOH, λ_{max}, nm ($\epsilon \times 10^{-3}$)): 301 (23.43), 413 (147.20), 546 (15.28), 585 (12.55). HRMS (FAB$^+$) *m*/*z* calcd for $C_{54}H_{55}N_5O^{64}Zn$: 853.3698. Found: 853.3683. MS (FAB$^+$), *m*/*z* (rel intensity): 859 (34), 858 (57), 857 (59), 856 (84), 855 (75), 854 (100) [M + H]$^+$, 815 (15), 814 (16), 813 (22), 812 (19), 811 (25) [M + H − COCH$_3$]$^+$. ^{1}H NMR (500 MHz, methylene-d_2 chloride): δ 10.14 (s, 2H, H10, H20), 10.06 (s, 1H, H15), 8.44 (bd, 1H, H4′, $J = 7.2$ Hz), 7.97 (d, 1H, H6′, $J = 7.0$ Hz), 7.86 (d, 1H, H7′ or H10′, $J = 7.5$ Hz), 7.63 (pseudo t, 1H, H5′, $J_{ave} = 7.6$ Hz), 7.56 (d, 1H, H10′ or H7′, $J = 7.2$ Hz), 7.35 (d, 1H, H1′, $J = 7.9$ Hz), 7.26 (pseudo t, 1H, H8′ or H9′, $J_{ave} = 7.5$ Hz), 7.18 (pseudo t, 1H, H9′ or H8′, $J_{ave} = 7.5$), 7.14 (d, 1H, H2′, $J = 7.9$ Hz), 4.05−3.94 (m, 12H, 2-, 8-, 12-, 13-, 17-, 18-β-CH_2CH$_3$), 3.86−3.93 (m, 2H, diastereotopic H, 3-, 7-β-CH_2CH$_3$), 3.74−3.82 (m, 2H, diastereotopic 3-, 7-β-CH_2-CH$_3$), 1.86, 1.85 (overlapping t, 12H, 12-, 13-, 17-, 18-β-CH$_2$CH_3, $J = 7.6$ Hz), 1.82 (t, 6H, 2-, 8-β-methyl, $J = 7.6$ Hz), 1.62 (s, 3H, COCH_3), 1.12 (t, 6H, 3-, 7-β-CH$_2$CH_3, $J = 7.6$ Hz).

c. 5-(*N*-1-Pyrenyl)acetamido-2,3,7,8,12,13,17,18-octaethylporphyrinatozinc(II) (3a). Compound **3a** was obtained in 18% yield. UV−vis (MeOH, λ_{max}, nm ($\epsilon \times 10^{-3}$)): 237 (15.09), 279 (8.96), 338 (11.29), 418 (72.51), 547 (4.72), 585 (3.61). HRMS (FAB$^+$) *m*/*z* calcd for $C_{54}H_{55}N_5O^{64}Zn$ [M$^+$]: 853.3698. Found: 853.3653. MS (FAB$^+$) *m*/*z* (rel intensity): 859 (17), 858 (33), 857 (58), 856 (56), 855 (82), 854 (78), 853 (92) [M$^+$], 814 (26), 813 (26), 812 (35), 811 (32), 810 (35) [M−COCH$_3$]$^+$, 601 (28), 600 (49), 599 (52), 598 (72), 597 (67), 596 (100) [M-acetamidopyrene]$^+$. ^{1}H NMR (500 MHz, methylene-d_2 chloride): δ 10.13 (s, 2H, H10, H20), 10.05 (s, 1H, H15), 8.75 (d, 1H, H10′, $J = 9.2$ Hz), 8.29 (overlapping: 2 × d, 2H, H9′, $J = 9.2$ Hz and H8′, $J = 7.4$ Hz), 8.19 (d, 1H, H6′, $J = 7.7$ Hz), 8.04 (pseudo t, 1H, H7′, $J_{ave} = 7.7$ Hz), 7.99 (d, 1H, H5′, $J = 8.6$ Hz), 7.83 (d, 1H, H4′, $J = 8.6$ Hz), 7.66 (d, 1H, H3′, $J = 8.9$ Hz), 7.59 (d, 1H, H2′, $J = 8.9$ Hz), 4.08−4.00 (m, 8H, 12-, 13-, 17-, 18-β-CH_2CH$_3$), 4.00−3.93 (m, 2H, diastereotopic 2-, 8-β-CH_2CH$_3$), 3.93−3.86 (m, 2H, diastereotopic 2-, 8-β-CH_2CH$_3$), 3.82−3.74 (m, 2H, diastereotopic 3-, 7-β-CH_2CH$_3$), 3.62−3.53 (m, 2H, diastereotopic 3-, 7-β-CH_2CH$_3$), 1.91−1.82 (overlapping, 2 × t at 1.86, 1.84, total 12H, 12-, 13-, 17-, 18-β-CH$_2$CH_3, $J = 7.6$ Hz), 1.78 (t, 6H, 2-, 8-β-CH$_2$CH_3, $J = 7.6$ Hz), 1.62 (s, 3H, COCH_3), 1.12 (t, 6H, 3-, 7-β-CH$_2$CH_3, $J = 7.6$ Hz).

General Procedure: 5-Arylamino-2,3,7,8,12,13,17,18-octaethylporphyrin. The zinc complex of the 5-arylaminoporphyrin obtained above was demetalated by stirring for 0.5 h in methylene chloride saturated with HCl. Removal of Zn(II) was accomplished quantitatively.

a. 5-*N*-Phenylacetamido-2,3,7,8,12,13,17,18-octaethylporphyrin (1b). UV−vis (MeOH, λ_{max}, nm ($\epsilon \times 10^{-3}$)): 236 (5.15), 398 (25.49), 503 (2.91), 537 (1.61), 573 (1.28), 627 (0.94). HRMS (FAB$^+$) *m*/*z* calcd for $C_{44}H_{53}N_5O$ [M$^+$]: 667.4250. Found: 667.4232. ^{1}H NMR (500 MHz, methylene-d_2 chloride): δ 10.15 (s, 2H, H10, H20), 9.97 (s, 1H, H15), 7.66 (d, 2H, phenyl *o*-H, $J = 7.7$ Hz), 7.07 (pseudo t, 2H, phenyl *m*-H, $J_{ave} = 7.7$ Hz), 6.94 (t, 1H, phenyl *p*-H, $J = 7.7$ Hz), 4.06−3.97 (m, 12H, 2-, 8-, 12-, 13-, 17-, 18-β-CH_2CH$_3$), 3.72−3.62 (m, 4H, 3-, 7-β-methylene), 1.9−1.8 (m, 18H, 2-, 8-, 12-, 13-, 17-, 18-β-CH$_2$CH_3), 1.62 (s, 3H, acetyl), 1.17 (t, 6H, 3-, 7-β- CH$_2$CH_3, $J = 7.5$ Hz), −3.27 (s, 1H, pyrrole N*H*), −3.33 (s, 1H, pyrrole N*H*).

b. 5-(*N*-3-Fluoranthenyl)acetamido-2,3,7,8,12,13,17,18-octaethylporphyrin (2b). Porphyrin **2b** was obtained in 35% yield directly from chromatographic purification of the coupling reaction product. UV−vis (MeOH, λ_{max}, nm ($\epsilon \times 10^{-3}$)): 299 (18.74), 405 (90.06), 507 (9.40), 540 (4.54), 576 (3.93), 628 (2.60). HRMS (FAB$^+$) *m*/*z* calcd for $C_{54}H_{57}N_5O$ [M$^+$]: 791.4563. Found: 791.4547. ^{1}H NMR (500 MHz, chloroform-*d*): δ 10.19 (s, 2H, H10, H20), 9.95 (s, 1H, H15), 8.61 (d, 1H, H4′, $J = 8.2$ Hz), 8.03 (d, 1H, H6′, $J = 6.9$ Hz), 7.90 (d, 1H, H7′ or H10′, $J = 7.6$ Hz), 7.78 (pseudo t, 1H, H5′, $J_{ave} = 7.7$ Hz), 7.61 (d, 1H, H10′ or H7′, $J = 7.2$ Hz), 7.37 (d, 1H, H1′, $J = 7.9$ Hz), 7.31 (pseudo t, 1H, H8′ or H9′, $J_{ave} = 7.5$ Hz), 7.24 (pseudo t [partially obscured by solvent protons], H9′ or H8′), 7.13 (d, 1H, H2′, $J = 7.9$ Hz), 4.12−3.98 (m, 12H, 2-, 8-, 12-, 13-, 17-, 18-β-methylene), 3.98−3.90 (m, 2H, diastereotopic 3-, 7-β-CH_2CH$_3$), 3.86−3.78 (m, 2H, diastereotopic 3-, 7-β-CH_2CH$_3$), 1.92−1.84 (overlapping, 3 × t at 1.91, 1.90, 1.87, 2-, 8-, 12-, 13-, 17-, 18-β-CH$_2$CH_3, $J = 7.6$ Hz, and s, 1H at 1.84, COCH_3, total 21H), 1.21 (t, 6H, 3-, 7-β-CH$_2$CH_3, $J_{ave} = 7.6$ Hz).

c. 5-(*N*-1-Pyrenyl)acetamido-2,3,7,8,12,13,17,18-octaethylporphyrin (3b). UV−vis (MeOH, λ_{max}, nm ($\epsilon \times 10^{-3}$)): 234 (20.9), 278 (10.79), 408 (32.79), 507 (2.86), 541 (1.82), 578 (1.79), 629 (1.05). HRMS (FAB$^+$) *m*/*z* calcd for $C_{54}H_{57}N_5O$ [M$^+$]: 791.4563. Found: 791.4519. ^{1}H NMR (500 MHz, methylene-d_2 chloride): δ 10.15 (s, 2H, H10, H20), 9.92 (s, 1H, H15), 8.72 (d, 1H, H10′, $J = 9.4$ Hz), 8.32 (d, 1H, H9′, $J = 9.4$ Hz), 8.31 (d, 1H, H8′, $J = 7.4$ Hz), 8.21 (d, 1H, H6′, $J = 7.6$ Hz), 8.06 (pseudo t, 1H, H7′, $J_{ave} = 7.6$ Hz), 8.02 (d, 1H, H5′, $J = 8.8$ Hz), 7.84 (d, 1H, H4′, $J = 8.8$ Hz), 7.69 (d, 1H, H3′, $J = 8.8$ Hz), 7.56 (d, 1H, H2′, $J = 8.8$ Hz), 4.07−3.90 (m, 12H, 2-, 8-, 12-, 13-, 17-, 18-β-CH_2CH$_3$), 3.79−3.71 (m, 2H, diastereotopic 3-, 7-β-CH_2CH$_3$), 3.60−3.52 (m, 2H, diastereotopic 3-, 7-β-CH_2CH$_3$), 1.850, 1.845 (overlapping: 2 × t, 12H, 12-, 13-, 17-, 18-β-CH$_2$CH_3, $J = 7.7$ Hz), 1.78 (t, 6H, 2-, 8-β-CH$_2$CH_3, $J = 7.7$ Hz), 1.77 (s, 3H, COCH_3), 1.15 (t, 6H, 3-, 7-β-CH$_2$CH_3, $J = 7.7$ Hz).

Chloro-5-*N*-phenylacetamido-2,3,7,8,12,13,17,18-octaethylporphyrinatoiron(III) (1c). To a degassed solution of 0.02 mmol porphyrin **1b** in 1:1 methanol/chloroform, 1 mmol ferrous chloride tetrahydrate was added, and the mixture was refluxed under argon for 2 min. The solvent was removed under reduced pressure and the solid residue chromatographed on silica eluted with 5% methanol in methylene chloride to remove inorganic salts. The complex was rechromatographed by TLC on alumina with methylene chloride eluant. The recovered product was converted to the chloro complex by treatment of a methylene chloride solution with HCl gas. Complex **1c** was obtained in >95% yield upon removal of solvent under reduced pressure. UV−vis (MeOH, λ_{max}, nm ($\epsilon \times 10^{-3}$)): 396 (81.4), 500 (6.18), 625 (3.30). HRMS (FAB$^+$) *m*/*z* calcd for $C_{44}H_{51}N_5O^{56}Fe$ [M$^+$]: 721.3443. Found: 721.3356. ^{1}H NMR (500 MHz, chloroform-*d*): δ 45.1, 44.7, 43.7, 43.2, 42.5, 40.0, 39.1, 38.1, 37.0 (1:2:1:1:2:4:3:1:1; 2, 3, 7-, 8-, 12-, 13-, 17-, 18-β-CH_2CH$_3$), 11.3, 10.2 (phenyl *o*-H), 6.90−5.70 (2-, 3-, 7-, 8-,12-, 13-, 17-, 18-β-CH$_2$CH_3 + OCH_3), −50.2, −60.7 (1:2, *meso*-H).

5-*N*-Phenyltrifluoroacetamido-2,3,7,8,12,13,17,18-octaethylporphyrin (4). Trifluoroacetanilide (0.5 mmol) in 10 mL of THF was stirred with NaH (1.0 mmol) under argon for 15 min. The resulting clear solution was added to a solution of Zn(II)OEP$^{\bullet+}$ generated from Zn(II)OEP (0.05 mmol) by treatment with tris(4-bromophenyl)aminium hexachloroantimonate (0.1 mmol) in 1:1 methylene chloride/THF solution. The green color of Zn(II)OEP$^{\bullet+}$ rapidly discharged, and the resulting purple solution was stirred for 3 h under argon. The solid remaining after evaporation of solvent under reduced pressure was chromatographed on silica eluted with 1:1 hexane/methylene chloride. Unreacted Zn(II)OEP was followed by **4**, which was isolated in 30% yield based on Zn(II)OEP. UV−vis (MeOH, λ_{max}, nm ($\epsilon \times 10^{-3}$)): 245

(17.36), 338 (27.64), 409 (196.4), 543 (17.78), 583 (22.64). MS (FAB^+) *m*/*z* (rel intensity): 788 (24), 787 (52), 786 (45), 785 (68), 784 (64), 783 (100) $[M]^+$, 597 (13), 596 (18) [M − trifluoroacetanilide]$^+$. ^1H NMR (500 MHz, chloroform-*d*): δ 10.20 (s, 2H, H10, H20), 10.14 (s, 1H, H15), 7.79 (bs, 2H, phenyl *o*-H), 7.25−7.16 (m, 2H, phenyl *m*-H), 7.11 (t, 1H, phenyl *p*-H, $J_{ave} = 7.1$ Hz), 4.11−4.02 (m, 12H, 2-, 8-, 12-, 13-, 17-, 18-β-CH_2CH$_3$), 3.78−3.65 (m, 4H, 3-, 7-β-CH_2CH$_3$), 1.95−1.87 (m, 18H, 2-, 8-, 12-, 13-, 17-, 18-β-CH$_2$CH_3), 1.09 (t, 6H, 3-, 7-β-CH$_2$CH_3, $J = 7.5$ Hz).

5-(*N*-3-Fluoranthenyl)trifluoroacetamido-2,3,7,8,12,13,17,18-octaethylporphyrinatozinc(II) (5). 3-Trifluoroacetamidofluoranthene (0.5 mmol) in 10 mL of THF was stirred with NaH (0.75 mmol) under argon for 15 min. The resulting clear solution was added to a solution of Zn(II)OEP$^{\bullet+}$ generated from Zn(II)OEP (0.05 mmol) by treatment with tris(*p*-bromophenyl)aminium hexachloroantimonate (0.1 mmol) in 1:1 methylene chloride/THF solution. The green color of the Zn(II)OEP$^{\bullet+}$ was rapidly discharged, and the resulting purple solution was stirred an additional 3 h under argon. After removal of the solvent under reduced pressure, the solid residue was chromatographed on silica eluted with 1:1 hexane/methylene chloride. The product was isolated in 30% yield (based on Zn(II)OEP) following elution of unreacted Zn(II)OEP and 3-trifluoroacetamidofluoranthene. UV−vis (MeOH, λ_{max}, nm ($\epsilon \times 10^{-3}$)): 216 (43.58), 300 (25.44), 416 (188.0), 547 (14.88), 585 (14.44). MS (FAB^+) *m*/*z* (rel intensity): 913 (10), 912 (28), 911 (55), 910 (53), 909 (69), 908 (73), 907 (100) $[M]^+$, 810 (10) [M − 3-trifluoroacetamidofluoranthene]$^+$. ^1H NMR (500 MHz, chloroform-*d*): δ 10.19 (s, 2H, H10, H20), 10.11 (s, 1H, H15), 8.41 (bs, 1H, H4′), 8.06 (d, 1H, H6′, $J = 6.9$ Hz), 7.91 (d, 1H, H7′, $J = 7.7$ Hz), 7.84 (bs, 1H, H5′), 7.63 (d, 1H, H10′, $J = 7.4$ Hz), 7.42 (d, 1H, H1′, $J = 8.0$ Hz), 7.34 (pseudo t, 1H, H8′ or H9′, $J_{ave} = 7.6$ Hz), 4.13−3.98 (m, 12H, 2-, 8-, 12-, 13-, 17-, 18-β-CH_2CH$_3$), 3.98−3.89 (m, 2H, diastereotopic 3-, 7-β-CH_2CH$_3$), 3.81−3.71 (m, 2H, diastereotopic 3-, 7-β-CH_2CH$_3$), 1.912, 1.905 (overlapping: 2 × t, 12H, 12-, 13-, 17-, 18-β-CH$_2$CH_3, $J = 7.5$ Hz), 1.87 (t, 6H, 2-, 8-β-CH$_2$CH_3, $J = 7.5$ Hz), 0.92 (t, 6H, 3-, 7-β-CH$_2$CH_3, $J = 7.5$ Hz).

General Procedure: Deacetylation of 5-(*N*-Aryltrifluoroacetamido)porphyrinatozinc(II) Derivatives. The porphyrinatozinc(II) complex (1 mmol) in 20 mL of 1:1 THF/methanol was refluxed with sodium methoxide (20 mmol) under argon for 1 h. Following removal of solvents under reduced pressure, the residue was taken up in methylene chloride and washed twice× with equal volumes of water. The organic layer was separated, dried over sodium sulfate, and evaporated to dryness under reduced pressure. The resulting solid was chromatographed by TLC on silica with 1:1 hexane/methylene chloride eluant.

a. 5-*N*-Phenylamino-2,3,7,8,12,13,17,18-octaethylporphyrinatozinc(II) (6a). Complex **6a** was isolated in 40% yield. UV−vis (MeOH, λ_{max}, nm ($\epsilon \times 10^{-3}$)): 243 (11.6), 331 (12.88), 414 (103.5), 545 (10.83), 579 (6.70). HRMS (FAB^+) *m*/*z* calcd for $C_{42}H_{49}N_5{}^{64}Zn$ $[M^+]$: 687.32794. Found: 687.33161. FAB/MS *m*/*z* (rel intensity): 692 (25), 691 (51), 690 (49), 689 (75), 688 (67), 687 (100), 686 (20) $[M]^+$. ^1H NMR (500 MHz, chloroform-*d*): δ 10.11 (s, 2H, H10, H20), 10.03 (s, 1H, H15), 7.85 (s, H, amino N*H*), 7.01 (bs, 2H, phenyl *m*-H), 6.69 (t, 1H, phenyl *p*-H, $J = 7.1$ Hz), 6.35 (bs, 2H, phenyl *o*-H), 4.08 (q, 8H, 12-, 13-, 17-, 18-β-CH_2CH$_3$, $J = 7.6$ Hz), 4.12 (m, 4H, 2-, 3-, 7-, 8-β-CH_2-CH$_3$), 3.81−3.73 (m, 2H, diastereotopic 3-, 7-β-CH_2CH$_3$), 1.92 (t, 12H, 12-, 13-, 17-, 18-β-CH$_2$CH_3, $J = 7.6$ Hz), 1.83 (t, 6H, 2-, 8-β-CH$_2$CH_3, $J = 7.6$ Hz), 1.74 (t, 6H, 3-, 7-β-CH$_2$CH_3, $J = 7.6$ Hz).

b. 5-(*N*-3-Fluoranthenyl)amino-2,3,7,8,12,13,17,18-octaethylporphyrinatozinc(II) (7a). Complex **7a** was obtained in 30% yield along with a trace quantity of the fused Zn(II) complex **9a**. UV−vis (MeOH, λ_{max}, nm (rel intensity)): 309 (0.18), 320 (0.19), 361 (0.20), 404 (1.00), 539 (0.12), 577 (0.10). HRMS (FAB^+) *m*/*z* calcd for $C_{52}H_{53}N_5{}^{64}Zn$ $[M^+]$: 811.35924. Found: 811.35000. ^1H NMR (500 MHz, chloroform-*d*): δ 10.15 (s, 2H, H10, H20), 10.09 (s, 1H, H15), 8.83 (s, 1H, amino N*H*), 8.63 (d, 1H, H4′, $J = 8.0$ Hz), 8.20 (d, 1H, H6′, $J = 7.1$ Hz), 7.99−7.92 (m, 2H, H5′, H7′), 7.55 (d, 1H, H10′, $J = 7.8$ Hz), 7.28−7.21 (overlapping with residual solvent protons, H8′, H9′), 7.11 (d, 1H, H1′, $J = 7.8$ Hz), 5.31 (d, 1H, H2′, $J = 7.8$ Hz), 4.15−4.02 (m, 10H, 2-, 8-, 12-, 13-, 17-, 18-β-CH_2CH$_3$), 4.02−3.95 (m, 2H, 2-, 8-β-CH_2CH$_3$), 3.95−3.87 (m, 2H, diastereotopic 3-, 7-β-CH_2CH$_3$), 3.75−3.66 (m, 2H, diastereotopic 3-, 7-β-CH_2CH$_3$), 1.94, 1.93 (overlapping 2 × t, 12H, 12-, 13-, 17-, 18-β-CH$_2$CH_3, $J = 7.6$ Hz), 1.82 (t, 6H, 2-, 8-β-CH$_2$CH_3, $J = 7.6$ Hz), 1.76 (t, 6H, 3-, 7-β-CH$_2$CH_3, $J = 7.6$ Hz).

General Procedure: 5-*N*-Arylaminoporphyrins from 5-*N*-Arylaminoporphyrinatozinc(II) Complexes. The Zn(II) complexes were quantitatively demetalated by stirring methylene chloride solutions for 15 min following addition of 5% v/v concentrated HCl. The methylene chloride solution was then washed with an equal volume of water and twice with equal volumes of saturated bicarbonate solution, dried over sodium sulfate, and evaporated under reduced pressure.

a. 5-*N*-Phenylamino-2,3,7,8,12,13,17,18-octaethylporphyrin (6b). UV−vis (MeOH, λ_{max}, nm ($\epsilon \times 10^{-3}$)): 240 (12.97), 405 (47.03), 507 (9.00), 535 (5.96), 575 (5.65), 618 (3.82). HRMS (FAB^+) *m*/*z* calcd for $C_{42}H_{51}N_5$ $[M^+]$: 625.4144. Found: 625.4086. ^1H NMR (500 MHz, chloroform-*d*): δ 10.06 (s, 2H, H10, H20), 9.88 (s, 1H, H15), 7.79 (s, 1H, amino N*H*), 7.06 (pseudo t, 2H, phenyl *m*-H, $J_{ave} = 7.4$ Hz), 6.75 (t, 1H, phenyl *p*-H, $J = 7.4$ Hz), 6.50 (bs, 2H, phenyl *o*-H), 4.12−3.98 (m, 12H, 2-, 8-, 12-, 13-, 17-, 18-β-CH_2CH$_3$), 3.98−3.88 (m, 2H, 3-, 7-β-CH_2CH$_3$), 3.78−3.68 (m, 2H, 3-, 7-β-CH_2CH$_3$), 1.91, 1.90 (overlapping 2 × t, 12H, 12-, 13-, 17-, 18-β-CH$_2$CH_3, $J = 7.6$ Hz), 1.81 (t, 6H, 2-, 8-β-CH$_2$CH_3, $J = 7.6$ Hz), 1.69 (t, 6H, 3-, 7-β-CH$_2$CH_3, $J = 7.6$ Hz), −3.12 (s, 2H, N*H*).

b. 5-*N*-(3-Fluoranthenyl)amino-2,3,7,8,12,13,17,18-octaethylporphyrin (7b) and 12-Azabenzo[*b*]fluorantheno[9,10,11-*tu*]-3,3,7,8,12,13,17,18-octaethyl-2H-porphyrin (9b). Demetalation of **7a** yielded two compounds, **7b** and **9b**, in 2:1 ratio, separated by TLC on silica with 3:1 hexane/methylene chloride eluant.

Porphyrin **7b**. UV−vis (CH_2Cl_2, λ_{max}, nm ($\epsilon \times 10^{-3}$)): 245 (19.39), 308 (13.04), 403 (46.33), 508 (7.94), 538 (2.92), 575 (3.58), 627 (1.24). HRMS (FAB^+) *m*/*z* calcd for $C_{52}H_{55}N_5$ $[M^+]$: 749.4457. Found: 749.4449. ^1H NMR (500 MHz, methylene-d_2 chloride): δ 10.15 (s, 2H, H10, H20), 10.00 (s, 1H, H15), 8.78 (s, 1H, amino N*H*), 8.66 (d, 2H, H4′, $J = 7.7$ Hz), 8.23 (d, 1H, H6′, $J = 7.1$ Hz), 8.02−7.96 (m, 2H, H5′, H10′), 7.59 (d, 1H, H7′, $J = 6.9$ Hz), 7.30−7.26 (m, 2H, H8′, H9′), 7.22 (d, 1H, H1′, $J = 7.8$ Hz), 5.57 (bd, 1H, H2′, $J = 7.8$ Hz), 4.15−4.14 (m, 10H, 2-, 8-, 12-, 13-, 17-, 18-β-CH_2CH$_3$), 4.04−3.95 (m, 2H, 2-, 8-β-CH_2CH$_3$), 3.89−3.80 (m, 2H, 3-, 7-β-CH_2CH$_3$), 3.75−3.65 (m, 2H, 3-, 7-β-CH_2CH$_3$), 1.92 (t, 12H, 12-, 13-, 17-, 18-β-CH$_2$CH_3, $J = 7.7$ Hz), 1.81 (t, 6H, 2-, 8-β-CH$_2$CH_3, $J = 7.7$ Hz), 1.70 (t, 6H, 3-, 7-β-CH$_2$CH_3, $J = 7.7$ Hz), −3.23 (bs, 2H, N*H*).

Porphyrin **9b**. UV−vis (MeOH, λ_{max}, nm ($\epsilon \times 10^{-3}$)): 234 (1.28), 359 (1.43), 437 (5.23), 451 (6.87), 574 (0.32), 625 (0.55), 683 (1.28). HRMS (FAB^+) *m*/*z* calcd for $C_{52}H_{53}N_5$ $[M^+]$: 747.4227. Found: 747.4301. ^1H NMR (500 MHz, methylene-d_2 chloride): δ 9.49 (d, 1H, H1′, $J = 8.0$ Hz), 9.19 (s, 1H, H8′), 9.08 (s, 1H, H15), 8.41 (s, 1H, H10), 8.33−8.30 (m, 1H, H7′), 8.25 (d, 1H, H3′), 8.10 (pseudo t, 1H, H2′, $J_{ave} = 8.3$ Hz), 8.09 (d, 1H, H4′, $J = 7.5$ Hz), 8.05 (s, 1H, H5), 7.60−7.53 (m, 2H, H5′, H6′), 4.58 (q, 2H, 18-β-CH_2CH$_3$, $J = 7.4$ Hz), 3.83 (q, 2H, 17-β-CH_2CH$_3$, $J = 7.5$ Hz), 3.64−3.56 (m, 4H, 7-, 8- or 12-β-CH_2CH$_3$), 3.54 (q, 2H, 13-β-CH_2CH$_3$, $J = 7.6$ Hz), 3.47 (q, 2H, 12- or 8-β-CH$_2$CH$_3$, $J = 7.5$ Hz), 3.36−3.27 (m, 2H, *gem*-β-CH_2CH$_3$), 3.13−3.05 (*gem*-β-CH_2CH$_3$), 2.02 (t, 3H, 18-β-CH$_2$CH_3, $J = 7.4$ Hz), 1.76 (t, 3H, β-CH$_2$CH_3, $J = 7.6$ Hz), 1.73 (t, 3H, 7-β-CH$_2$CH_3, $J = 7.6$ Hz), 1.71 (t, 3H, β-CH$_2$CH_3, $J = 7.6$ Hz), 1.67 (t, 3H, 13- or 17-β-CH$_2$CH_3, $J = 7.6$ Hz), 1.64 (t, 3H, 8- or 12-β-CH$_2$CH_3, $J = 7.6$ Hz), −0.01 (t, 6H, *gem*-β-CH$_2$CH_3, $J = 7.3$ Hz).

Chloro-5-*N*-Phenylamino-2,3,7,8,12,13,17,18-octaethylporphyrinatoiron(III) (6c). A total of 0.7 mmol of ferrous chloride tetrahydrate was added to a degassed solution of 0.024 mmol of porphyrin **6b** in 1:1 methanol/chloroform (20 mL). The reaction mixture was stirred under a nitrogen atmosphere for 10 min at ambient temperature and partitioned between chloroform and water. The organic layer was dried over sodium sulfate and evaporated to dryness under reduced pressure. The solid residue was flash-chromatographed over silica. Elution with 1:1 hexane/methylene chloride yielded the fused metal-free base **8a** (see below). Further elution with 5% MeOH in chloroform gave meso-substituted iron complex **6c** in 25% yield based on starting porphyrin. UV−vis (MeOH, λ_{max}, nm ($\epsilon \times 10^{-3}$)): 270 (11.07), 353 (19.97), 404 (29.51), 563 (4.42). HRMS (FAB^+) *m*/*z* calcd for $C_{42}H_{49}N_5{}^{56}Fe$ $[M^+]$: 679.3337. Found: 679.3271. ^1H NMR (500 MHz, chloroform-*d*): δ 43.5, 43.3, 42.1, 40.0, 39.7, 39.4, 38.6, 37.2 (2:2:4:2:1:1:1:4, 2-, 3-,

7-, 8-, 12-, 13-, 17-, 18-β-CH_2CH_3 + N*H*), 6.58, 6.23, 5.84 (2-, 3-, 7-, 8-, 12-, 13-, 17-, 18-β-CH_2CH_3), −57.1 (H15), −61.2 (H10, H20).

Quinolino[2,3,4-*tu*]-3,3,7,8,12,13,17,18-octaethyl-2*H*-porphyrin (8a). Porphyrin **8a** was obtained in 25% yield from metalation of porphyrin **6b** described above. UV−vis (MeOH, λ_{max}, nm ($\epsilon \times 10^{-3}$)): 270 (4.49), 354sh (7.08), 409 (17.99), 425sh (12.66), 450sh (3.97), 550 (1.25), 595 (1.42), 629 (2.05), 687 (4.06). HRMS (FAB^+) *m*/*z* calcd for $C_{42}H_{48}N_5$ [$(M - H^{\bullet})^+$]: 622.4056. Found: 622.3910. ^{1}H NMR (600 MHz, chloroform-*d*): δ 8.81 (d, 1H, H8′, J = 8.5 Hz), 8.73 (s, 1H, H15), 8.70 (d, 1H, H5′, J = 8.5 Hz), 8.00 (s, 1H, H10), 8.01−7.97 (s, overlapping with pseudo triplet, 2H, H10, H7′), 7.84 (pseudo t, 1H, H6′, J_{ave} = 7.5 Hz), 7.59 (s, 1H, H5′), 4.20 (q, 2H, 18-β-CH_2CH_3, J = 7.4 Hz), 3.61 (q, 2H, 17-β-CH_2CH_3, J = 7.6 Hz), 3.42−3.34 (m, 6H, 7-, 12- or 8-, 13-β-CH_2CH_3), 3.30 (q, 2H, 8- or 12-β-CH_2CH_3, J = 7.4 Hz), 3.07−2.99 (m, 2H, *gem*-β-CH_2CH_3), 2.86−2.78 (m, 2H, *gem*-β-CH_2CH_3), 1.79 (t, 3H, 18-β-CH_2CH_3, J = 7.4 Hz), 1.65−1.58 (m, 15H, 7-, 8-, 12-, 13-β-CH_2CH_3), 0.09 (t, 6H, *gem*-β-CH_2CH_3, J = 7.4 Hz).

Chloroquinolino[2,3,4-*tu*]-3,3,7,8,12,13,17,18-octaethyl-2*H*-porphyrinatoiron(III) (8b). To a degassed solution of 0.0074 mmol of porphyrin **6b** in 1:1 methanol/chloroform (20 mL), 1.3 mmol of ferrous chloride tetrahydrate was added, and the reaction mixture was refluxed under argon for 5 min. The solvents were removed under reduced pressure and the residue chromatographed on silica with 4% MeOH in methylene chloride as eluant. Final purification was accomplished by TLC on silica with methylene chloride eluant. Following removal from the plate, the iron complex was dissolved in methylene chloride and treated with HCl gas for complete conversion to the chloro form. Complex **8b** was obtained in 75% yield based on porphyrin **6b**. UV−vis (MeOH, λ_{max}, nm ($\epsilon \times 10^{-3}$)): 275 (28.85), 414 (79.94), 546 (8.04), 629 (7.29), 686 (9.07). HRMS (FAB^+) *m*/*z* calcd for $C_{42}H_{47}N_5{}^{56}Fe$ [M^+]: 677.3180. Found: 677.3211. ^{1}H NMR (600 MHz, chloroform-*d*): δ 59.6, 51.4, 51.0, 50.8, 49.5, 49.2, 43.9, 43.5, 42.4, 40.1, 37.4 (1:1:1:1:1:1:1:1:2, 7-, 8-, 12-, 13-, 17-, 18-β-CH_2CH_3), 33.8, 32.6 (*gem*-β-CH_2CH_3), 18.9, 17.6 (quinolino H′), 10.2, 8.8 (*gem*-β-CH_2CH_3), 6.5, 6.1, 5.8 (β-CH_2CH_3), −1.4 (β-CH_2CH_3), −5.5, −11.9 (quinolino H′), −21.3, −84.4 (*meso*-H).

Chloro-12-Azabenzo[*b*]fluorantheno[9,10,11-*tu*]-3,3,7,8,12,13,17,18-octaethyl-2*H*-porphyrinatoiron(III) (9c). To a degassed solution of porphyrin **7b** (0.0045 mmol) in 1:1 methanol/chloroform (20 mL) was added 0.615 mmol of ferrous sulfate tetrahydrate. The reaction was refluxed under argon for 20 min, and the solvent was evaporated under reduced pressure. The solid residue was chromatographed on silica eluted with 4% methanol in chloroform. Final purification was achieved by TLC on alumina eluted with methylene chloride. The desorbed product was dissolved in methylene chloride and treated with HCl gas to ensure complete conversion to chloro complex **9c**, obtained in 70% yield based on starting porphyrin **7b**. UV−vis (MeOH, λ_{max}, nm ($\epsilon \times 10^{-3}$)): 263 (17.08), 350 (14.41), 437 (37.28), 593 (3.80), 638 (4.07). HRMS (FAB^+) *m*/*z* calcd for $C_{52}H_{53}N_5{}^{56}Fe$ [M^+]: 801.3697. Found 801.3775. ^{1}H NMR (500 MHz, chloroform-*d*): δ 59.6, 50.8, 50.3, 49.0, 48.1, 44.1, 43.5, 42.9, 40.8, 38.8, 38.1 (1:1:1:2:1:1:1:1:1:1:1, 7-, 8-, 12-, 13-, 17-, 18-β-CH_2CH_3), 34.8, 33.3 (*gem*-β-CH_2CH_3), 11.6 (12-azabenzo[*b*]fluoranthene H′), 10.7 (3-β-CH_2CH_3), 9.6 (12-azabenzo[*b*]fluorantheno H′), 9.5 (*gem*-β-CH_2CH_3), 8.8, 8.2 (12-azabenzo[*b*]fluorantheno H′), 6.7, 6.5, 5.9 (β-CH_2CH_3), −1.3 (*gem*-β-CH_2CH_3), −26.7, −76.0 (*meso*-H).

1-(2,4-Dinitrobenzenesulfonamido)pyrene. 2,4-Dinitrobenzenesulfonyl chloride (1.35 mmol) in methylene chloride (4 mL) was added slowly with stirring to a solution of 1-aminopyrene (1.4 mmol) and pyridine (1.5 mmol) in methylene chloride (6 mL). After being stirred for an additional 15 min, the reaction mixture was washed twice× with water, the organic layer dried over sodium sulfate, and the solvent evaporated under reduced pressure. The residue was flash-chromatographed on silica eluted with methylene chloride. EI/MS *m*/*z* (rel intensity): 447 (3.7) $[M]^+$, 217 (100) [M − 2,4-dinitrobenzenesulfonyl]$^+$.

10-Azabenzo[*a*]pyreno[7,8,9-*tu*]-3,3,7,8,12,13,17,18-octaethyl-2*H*-porphyrin (10a). 1-(2,4-Dinitrobenzenesulfonamido)pyrene (0.3 mmol) in THF (10 mL) was stirred for 10 min with NaH (1.2 mmol) at 42 °C under argon. This solution was added to a solution of $Zn(II)OEP^{\bullet+}$ (0.05 mmol) generated from Zn(II)OEP (0.05 mmol) with tris(4-bromophenyl)aminium hexachloroantimonate (0.1 mmol) in 1:1 methylene chloride/THF. The reaction was stirred for 3 h at ambient temperature under argon. Following evaporation of the solvent under reduced pressure, the residue was chromatographed on silica. Unreacted Zn(II)OEP was eluted with 1:1 hexane/methylene chloride, and the Zn(II) complex of the porphyrin **10a** followed on elution with methylene chloride. The crude product was demetalated by stirring 5% v/v methylene chloride/concentrated HCl, and the porphyrin was purified by TLC on silica eluted with 2:1 hexane/methylene chloride. The yield of purified **10a** was 5% based on starting Zn(II)OEP. UV−vis (MeOH, λ_{max}, nm ($\epsilon \times 10^{-3}$)): 240 (5.04), 341 (4.85), 420 (7.17), 439 (7.25), 465 (7.99) 598 (1.13), 6.52 (1.19), 716 (1.70). HRMS (FAB^+) *m*/*z* calcd for $C_{52}H_{53}N_5$ [M^+]: 747.4301. Found: 747.4210. ^{1}H NMR (500 MHz, chloroform-*d*): δ 10.35 (d, 1H, H11′, J = 8.9 Hz), 9.28 (s, 1H, H6′), 8.82 (s, 1H, H15), 8.65 (d, 1H, H12′, J = 8.9 Hz), 8.40 (d, 1H, H1′, J = 7.8 Hz), 8.27 (d, 1H, H3′, J = 9.0 Hz), 8.18 (d, 1H, H4′, J = 7.3 Hz), 8.08−8.05 (m, 3H, H2′, H5′, H10), 7.75 (s, 1H, H5), 4.58 (q, 2H, 18-β-CH_2CH_3, J = 7.4 Hz), 3.73 (q, 2H, 17-β-CH_2CH_3, J = 7.6 Hz), 3.50−3.39 (m, 6H, 7-, 8- or 12-, 13-β-CH_2CH_3), 3.38−3.29 (m, 4H, *gem*-, 12- or 8-β-CH_2CH_3), 3.04−2.95 (m, 2H, *gem*-β-CH_2CH_3), 2.04 (t, 3H, 18-β-CH_2CH_3, J = 7.4 Hz), 1.72 (t, 3H, 17-β-CH_2CH_3, J = 7.6 Hz), 1.67 (t, 3H, 7-β-CH_2CH_3, J = 7.6 Hz), 1.65 (t, 3H, 8- or 12-β-CH_2CH_3, J = 7.7 Hz), 1.61 (t, 3H, 13-β-CH_2CH_3, J = 7.6 Hz), 1.57 (t, 3H, 12- or 8-β-CH_2CH_3, J = 7.7 Hz), −0.03 (t, 6H, *gem*-β-CH_2CH_3, J = 7.4 Hz).

Chloro-10-Azabenzo[*a*]pyreno[7,8,9-*tu*]-3,3,7,8,12,13,17,18-octaethyl-2*H*-porphyrinatoiron(III) (10b). Ferrous chloride tetrahydrate (1.45 mmol) was added to a degassed solution of porphyrin **10a** (0.007 mmol) in 1:1 methanol/chloroform, and the reaction was refluxed for 6 min. Following removal of solvent under reduced pressure, the residue was chromatographed on silica. A small quantity of **10a** was eluted with methylene chloride, and the ferric complex **10b** was eluted with 10% methanol in methylene chloride. The iron complex was further purified by TLC on silica eluted with methylene chloride. The recovered product was treated in methylene chloride with HCl gas to conversion to the chloro complex **10b**, obtained in 90% yield from **10a**. UV−vis (MeOH, λ_{max}, nm ($\epsilon \times 10^{-3}$)): 258 (14.41), 280 (13.94), 340 (16.49) 437 (35.81), 642 (4.31), 702 (4.03). HRMS (FAB^+) *m*/*z* calcd for $C_{52}H_{51}N_5{}^{56}Fe$ [M^+]: 801.3493. Found 801.3448. ^{1}H NMR (500 MHz, methylene-d_2 chloride): δ 59.7, 51.2, 49.6.49.4, 49.0, 43.8, 42.8, 41.0, 38.2, 37.5 (1:2:1:1:1:2:1:1:1:1, 7-, 8-, 12-, 13-, 17-, 18-β-CH_2CH_3), 33.8, 32.9 (*gem*-β-CH_2CH_3), 12.1, 10.8, 10.6, 10.3 (10-azabenzo[*a*]pyreno H′), 9.1, 8.7 (*gem*-β-CH_2CH_3), 7.3 (β-CH_2CH_3), 6.6 (10-azabenzo[*a*]pyreno H′), 6.5 (β-CH_2CH_3), 5.9 (β-CH_2CH_3), 4.6 (10-azabenzo[*a*]pyreno H′), 3.1 (β-CH_2CH_3), −1.3 (*gem*-β-CH_2CH_3), −3.8 (10-azabenzo[*a*]pyreno H′), −23.8 (*meso*-H), −81 (*meso*-H).

Acknowledgment. This work was supported by USEPA Grant R825346.

Supporting Information Available: ^{1}H NMR spectra of all metal-free bases and Zn(II) and Fe(III) complexes and listings of crystallographic details, atomic coordinates, anisotropic temperature factors, fixed hydrogen atom positions, and bond distances and angles for complexes **9c** and **10b**. This material is available free of charge via the Internet at http://pubs.acs.org.

IC000112R